Gene expression dynamics and inter-tissue recognition mechanisms during tissue fusion at the *Arabidopsis* graft junction

Charles W Melnyk[1,2], Alexander Gabel[3], Thomas J Hardcastle[4], Sarah Robinson[5], Shunsuke Miyashima[6], Ivo Grosse[3], Elliot M Meyerowitz[1,7]

1- Sainsbury Laboratory, University of Cambridge, Bateman Street, Cambridge CB2 1LR, UK
2 – Department of Plant Biology, Swedish University of Agricultural Sciences, Almas allé 5, 756 51 Uppsala, Sweden
3 - Institute of Computer Science, Martin Luther University Halle–Wittenberg, 06120 Halle (Saale), Germany
4 – Department of Plant Sciences, University of Cambridge, Downing Street, Cambridge CB2 3EA, United Kingdom
5 - Institute of Plant Science, University of Bern, Altenbergrain 21, 3013 Bern, Switzerland
6 – Graduate School of Biological Sciences, Nara Institute of Science and Technology, 8916-5 Takayama, Ikoma, Nara 630-0192, Japan
7 – Howard Hughes Medical Institute and Division of Biology and Biological Engineering, California Institute of Technology, 1201 East California Boulevard, Pasadena, CA 91125, USA

Contact: charles.melnyk@slu.se

ABSTRACT

The ability for cut tissues to join together and form a chimeric organism is a remarkable and agriculturally important property of many plants, however, it is poorly characterized at the molecular level. To better understand grafting we monitored temporal and spatial changes in gene expression in grafted tissues. Tissues above and below the graft rapidly developed asymmetry such that many genes were more highly expressed on one side than the other. This asymmetry correlated with sugar responsive genes and we observed an accumulation of starch above the graft that, after three days, decreased along with asymmetry once vascular connections were re-established. Despite an initial starvation response below the graft, many genes associated with cell division and vascular formation were rapidly activated in grafted tissues but not in cut and separated tissues indicating a recognition mechanism that was independent of functional vascular connections. Auxin response in grafted plants differed from that in cut and separated plants as response was enhanced and symmetric, suggesting that auxin was perceived by the root within hours of reattachment to activated vascular regeneration. Such a recognition process could have broader relevance for wound healing, inter-tissue communication and tissue fusion events.

INTRODUCTION

For millennia people have cut and rejoined plants through grafting. Generating such chimeric organisms combines desirable characteristics from two plants, such as disease resistance, dwarfing and high yields, or can propagate plants and avoid the delays entailed by a juvenile state (Goldschmidt, 2014). Agriculturally, grafting is becoming more relevant as a greater number of plants and species are grafted to increase productivity and yield (Lee et al., 2010). However, our mechanistic understanding of grafting and the biological processes involved, including wound healing, tissue fusion and vascular formation, remain limited.

Plants have efficient mechanisms to heal wounds and cuts, in part through the production of wound-induced pluripotent cells termed callus. The callus fills the gap or seals the wound, and later, differentiates to form epidermal, mesophyll

67 and vascular tissues (Melnyk, 2017c). In grafted *Arabidopsis* hypocotyls, tissues
68 adhere 1-2 days after grafting and the phloem, the tissue that transports sugars
69 and nutrients, connects after three days (Yin et al., 2012; Melnyk et al., 2015).
70 The xylem, tissue that transports water and minerals, connects after seven days
71 (Melnyk et al., 2015). Plant hormones are important regulators of vascular
72 formation, and at the graft junction, both auxin and cytokinin responses increase
73 in the vascular tissue (Yin et al., 2012; Melnyk et al., 2015; Matsuoka et al., 2016).
74 Auxin is important for differentiation of vascular tissues whereas cytokinin
75 promotes vascular stem cells, termed cambium, to divide and proliferate in a
76 process known as secondary growth (Matsumoto-Kitano et al., 2008; Leyser,
77 2011). Auxin is produced in the upper parts of a plant and moves towards the
78 roots via cell-to-cell movement. Auxin exporters, including the PIN proteins,
79 transport auxin into the apoplast, whereas auxin importers, such as the AUX and
80 LAX proteins, assist with auxin uptake into adjacent cells (Leyser, 2011).
81 Disrupting this transport, such as by mutating *PIN1*, inhibits healing of a
82 wounded stem (Asahina et al., 2011). Blocking auxin transport with the auxin
83 transport inhibitor TIBA (2,3,5-triiodobenzoic acid) in the shoot inhibits vascular
84 formation and cell proliferation at the *Arabidopsis* graft junction (Matsuoka et al.,
85 2016). In addition to auxin, other compounds, including sugars, contribute to
86 vascular formation. The localised addition of auxin to callus induces phloem and
87 xylem but requires the presence of sugar (Wetmore & Rier, 1963; Aloni, 1980).
88 In plants, sugars are produced in the leaves and transported through the phloem
89 to the roots (Lough & Lucas, 2006). The role of sugars in vascular formation and
90 wound healing is not well established, however, sugars promote cell division and
91 cell expansion (Wang & Ruan, 2013), processes important for development
92 including vascular formation.
93
94 The molecular and cellular mechanisms for wound healing, tissue reunion and
95 graft formation remain largely unknown. One emerging theme is that the top and
96 bottom of the cut do not behave similarly. Such tissue asymmetry occurs in other
97 plant tissues, most notably leaves. Developing leaf primordia have an inherent
98 asymmetry that is thought to derive from positional signals from the shoot apical
99 meristem that specifies differences between the top and the bottom of the leaf.

100 The molecular mechanisms that establish asymmetry are not well described,
101 though one hypothesis is that auxin contributes towards or acts on the putative
102 signal (Chitwood et al., 2007). Asymmetry also appears in cut *Arabidopsis*
103 inflorescence stems where the transcription factor *RAP2.6L* expresses
104 exclusively below the cut whereas the transcription factor *ANAC071* expresses
105 exclusively above the cut (Asahina et al., 2011). Both were important for stem
106 healing and *ANAC071* and a close homologue, *ANAC096*, were important for graft
107 formation (Matsuoka et al., 2016). Asymmetry also exists in genetic
108 requirements, since *ALF4* and *AXR1*, two genes involved in auxin perception, are
109 important below but not above the graft junction for phloem connection (Melnyk
110 et al., 2015). However, *ANAC071* is expressed symmetrically around the
111 hypocotyl graft junction three days after grafting (Matsuoka et al., 2016) so the
112 extent of asymmetry and the mechanistic basis for it during wound healing
113 remains largely uncharacterised.
114
115 Previous efforts have characterised wound healing and tissue reunion using
116 transcriptomic analyses. Mechanical wounding altered approximately 8% of the
117 *Arabidopsis* transcriptome and showed a high degree of overlap with
118 transcriptomic changes elicited by pathogen attack and abiotic stress (Cheong et
119 al., 2002). Stem wounding and wound-induced callus formation altered the
120 expression of hundreds or thousands of genes (Asahina et al., 2011; Iwase et al.,
121 2011; Ikeuchi et al., 2017), whereas grafting grape vines, lychee trees and
122 hickory trees induced hundreds or thousands of differentially expressed genes
123 involved in hormone response, wound response, metabolism, cell wall synthesis
124 and signal transduction (Zheng et al., 2010; Yin et al., 2012; Cookson et al., 2013;
125 Cookson et al., 2014; Chen et al., 2017). These grafting studies provide limited
126 information, as tissues from above and below the graft junction were not isolated
127 to test whether these tissues behaved differently, and controls were not
128 performed to distinguish how grafting and tissue fusion might differ from a
129 response associated with cut tissues that remained separated. Here, we perform
130 an in-depth analysis to describe the spatial and temporal transcriptional
131 dynamics that occur during healing of cut *Arabidopsis* tissues that are joined
132 (grafted) or left unjoined (separated). We find that the majority of genes

133 differentially expressed are initially asymmetrically expressed at the graft
134 junction and that many of these genes are sugar responsive, which correlates
135 with severing of the phloem tissue and the accumulation of starch above the
136 junction. However, genes associated with cell division and vascular formation
137 activate on both sides of the graft and, similarly, auxin responsiveness activates
138 equally on both sides. We propose that the continuous transport of substances,
139 including auxin, independent of functional vascular connections, promoted
140 division and differentiation, while the enhanced auxin response and blocked of
141 sugar transport provided a unique physiological condition to activate genes
142 specific to graft formation that promote wound healing.
143
144 **RESULTS**
145 **Genes are asymmetrically expressed around the graft**
146 Previous analyses revealed an asymmetry in the genetic requirements for tissue
147 reunion or graft formation and identified several genes expressed above a cut
148 that were not expressed below (Asahina et al., 2011; Melnyk et al., 2015). To
149 investigate whether asymmetry was a common feature of grafting and tissue
150 reunion, we generated RNA deep sequencing libraries from *Arabidopsis thaliana*
151 hypocotyl tissues immediately above and immediately below the graft junction 0,
152 6, 12, 24, 48, 72, 120, 168 and 240 hours after grafting (HAG)(Figure 1A). Prior
153 to RNA extraction, we separated top and bottom tissues at the graft junction. We
154 found that the strength required to break apart the graft junction increased
155 linearly (Figure S1) similarly to previously reported breaking strength dynamics
156 of grafted *Solanum pennellii* and *Solanum lycopersicum* (Lindsay et al., 1974;
157 Moore, 1984). When pulling apart grafts to separate top and bottom for sample
158 preparation, grafts broke cleanly with minimal tissue from one half present in
159 the other half (Figure S1, Movie S1, S2). We measured the amount of tissue from
160 tops adherent to bottoms and *vice versa* (Figure S1) and found less than 4%
161 cross-contamination. In addition to grafting, we also prepared libraries from
162 ungrafted hypocotyls ("intact" treatment) and cut plants that had not been
163 reattached ("separated" treatment)(Figure 1A). We herein refer to tissues
164 harvested above the graft junction or from the shoot side of separated tissue as

165 “top” and that from below the graft or from the root side of separated tissue as
166 “bottom” (Figure 1A).
167
168 RNAs that were differentially expressed as a consequence of grafting (compared
169 to intact hypocotyls) equally in tops and bottoms of grafts (symmetrically
170 expressed) or were more highly expressed in one tissue than the other
171 (asymmetrically expressed), were identified by performing a pairwise analysis of
172 the protein-coding transcriptome datasets that were differentially expressed
173 relative to the intact group. Several thousand RNAs were identified that fit either
174 pattern of expression including the transcript of the cambial markers *HCA2* that
175 was induced symmetrically, and *ANT* that was induced asymmetrically (Figure
176 1B-G, Figure S2). 6 to 48 hours after grafting, the number of graft-differentially
177 expressed genes that were asymmetrically expressed was roughly 3-fold greater
178 than those symmetrically expressed indicating that tissues above the cut
179 changed their expression dynamics relative to below the cut. However, at 72
180 hours the numbers were nearly equal, and by 120 hours, the number of
181 symmetrically differentially expressed genes was 3-fold greater than those
182 asymmetrically expressed (Figure 1B). As a second approach, we performed a
183 hierarchical clustering analysis that indicated that the grafted top and grafted
184 bottom became most similar after 72 hours (Figure S3), consistent with the
185 symmetry analysis (Figure 1B). Thus, graft healing and tissue reunion promoted
186 a shift from asymmetry to symmetry (Figure 1B).
187

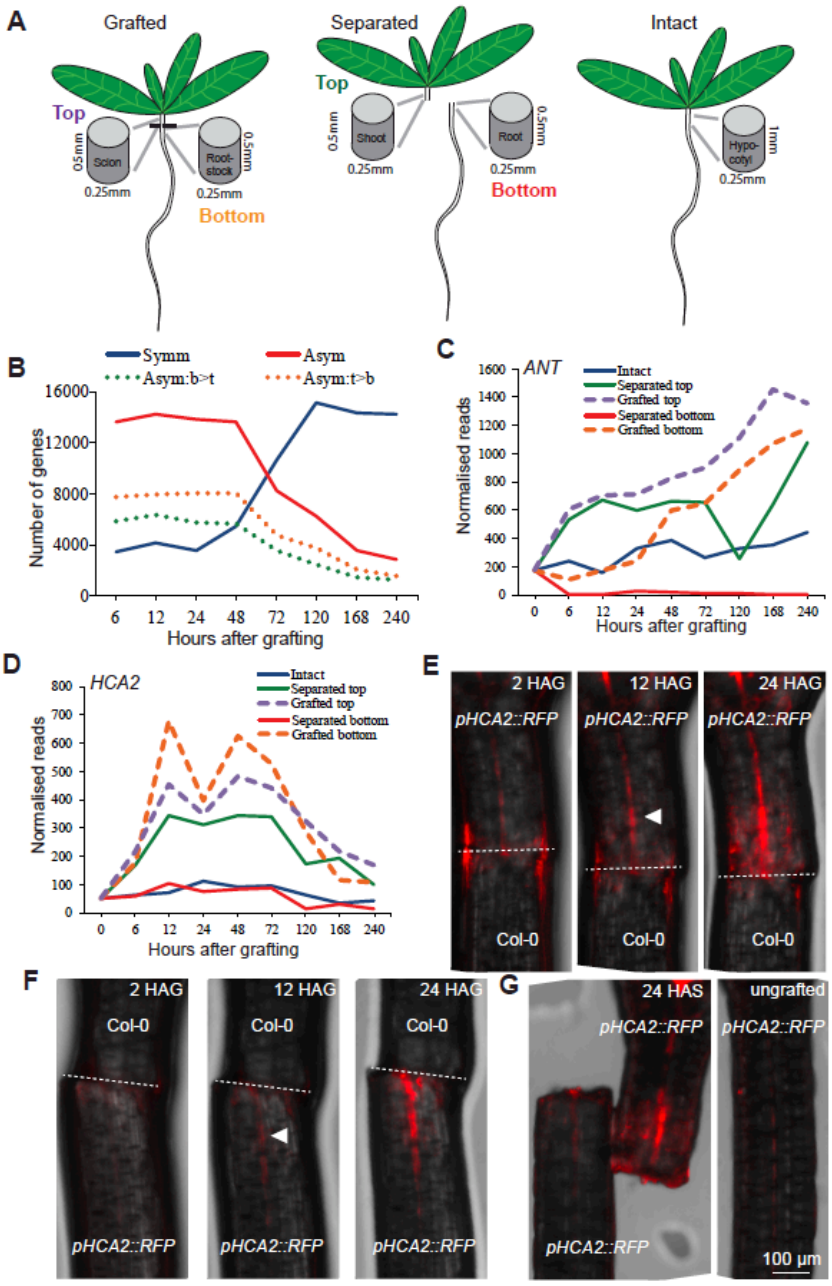

Figure 1. Grafting rapidly activates genes in both asymmetric and symmetric patterns. (A) Intact, cut and separated, or cut and grafted *Arabidopsis* tissues were harvested approximately 0.5mm above (top), 0.5mm below (bottom) the cut site or for intact plants 1mm segments spanning the region where cuts were made in grafted and separated plants. (B) Pairwise analysis between the grafted top and grafted bottom identified sets of protein-coding genes symmetrically or asymmetrically expressed at the graft junction, with an FDR < 0.05 and a likelihood of symmetric/asymmetric expression of greater than 50%. Asymmetrically expressed genes were further divided into those whose RNAs were higher in the top (orange dotted line) or higher in the bottom (purple dotted line), again with an FDR < 0.05 and a likelihood of asymmetric expression greater than 50%. (C,D) Expression profiles for transcripts of cambium-associated genes that initially activate symmetrically (*HCA*) or asymmetrically (*ANT*) plotted for intact, separated and grafted samples.

203 (E-G) *HCA2* transcription upregulates above the graft junction (E) and below the
204 graft junction. (F) *pHCA2::RFP* was grafted to Col-0 roots (E) or Col-0 shoots (F)
205 to avoid ambiguity of signal origin at the junction. *HCA2* was also upregulated in
206 separated shoots but not in intact samples or in high levels in separated roots
207 (G). HAG, hours after grafting. HAS, hours after separation. White triangle
208 denotes initial fluorescent signal, dashed lines denote the graft junction.
209
210 **Sugar response correlates with asymmetric gene expression**
211 The shift from asymmetry to symmetry could be due to phloem reconnection at
212 72 hours ((Melnyk et al., 2015), Figure 2A) and the resumption of hormone,
213 protein and sugar transport. We tested a role for sugar by grafting in the
214 presence of exogenous sucrose which has previously been reported to affect
215 grafting success (Marsch-Martinez et al., 2013). Low levels of exogenous sucrose
216 lowered grafting efficiency (Figure 2A), suggesting that differential sugar
217 responses at the graft junction might be important for vascular reconnection.
218 Expression of *ApL3*, a gene whose expression is induced by sugar (Villadsen &
219 Smith, 2004), was rapidly upregulated in separated tops and grafted tops,
220 whereas expression of *DIN6*, *GDH1* and *STP1*, genes whose expression is
221 repressed by sugar (Thum et al., 2004; Villadsen & Smith, 2004; Cordoba et al.,
222 2015), was rapidly upregulated in separated bottoms and grafted bottoms
223 (Figure 2B, Figure S4). These observations were consistent with sugar
224 accumulation in the grafted top and sugar depletion in the grafted bottom. The
225 expression of these genes returned to levels similar to intact samples by 120
226 hours and, with the exception of *ApL3*, the grafted samples normalised
227 expression more rapidly than the separated tissues. Genes associated with
228 photosynthesis increase expression in separated bottoms 24 hours after cutting,
229 a common response to starvation (Wang & Ruan, 2013), but likely too late to
230 affect sugar levels before 24 hours (Figure S4). A transcriptional overlap analysis
231 with RNAs from known glucose-responsive genes (Table S1) revealed a strong
232 overlap with genes differentially expressed by grafting. RNAs from known
233 glucose-induced genes were upregulated in separated tops and grafted tops,
234 whereas transcripts from known glucose-repressed genes were upregulated in
235 separated bottoms and grafted bottoms (Figure 2C, Figure S4). This trend was
236 not observed with genes differentially expressed by mannitol treatment (Figure
237 S4), suggesting the effect was specific to metabolically active sugars. To further

238 investigate this effect, we stained grafted, separated and intact plants with Lugol
239 solution to assay for the presence of starch. Staining above the graft junction
240 increased 48-72 hours after grafting (Figure 2D). By 120 hours, staining was
241 equal on both sides of the graft whereas in separated tops staining became
242 stronger after 72 hours (Figure 2D, Figure S4). We concluded that starch
243 accumulated above the graft junction, but after 72 hours, this asymmetry
244 disappeared. To test whether the accumulation of starch and increased sugar
245 responsiveness could explain the observed transition from asymmetry to
246 symmetry, we compared our datasets to previously published genes that are
247 induced by starvation or are induced by sucrose re-addition (Table S1). In early
248 time points, 20-31% of asymmetrically expressed genes are genes known to
249 respond to sugars compared to 2-5% of symmetrically expressed genes (Table
250 1). However, at 72 hours, the overlap between asymmetrically expressed genes
251 and sugar responsive genes reduced substantially (Table 1).

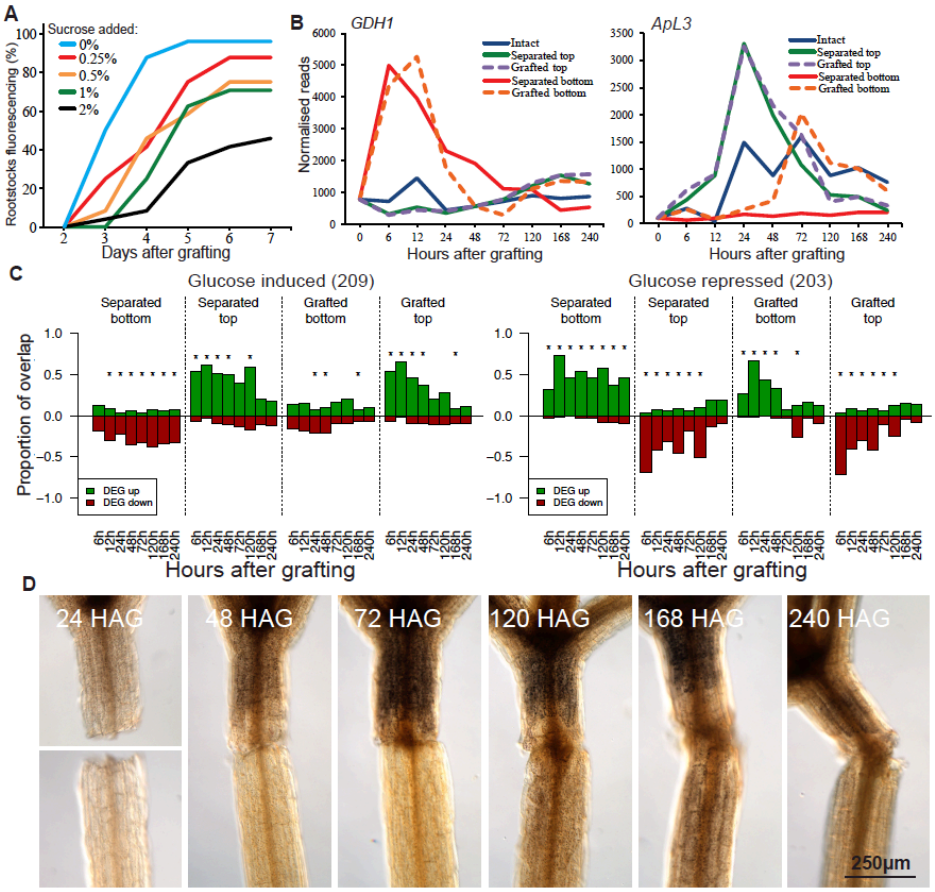

252

253 **Figure 2. Asymmetric changes in accumulation of sugar-responsive RNAs**
254 **and of starch occur at the graft junction; equalizing sucrose between the**
255 **grafted segments reduces and delays phloem reconnection.** (A) *pSUC2::GFP*-
256 expressing *Arabidopsis* shoots were grafted to Col-0 wild type roots and GFP

257 movement to the roots was monitored over 7 days for phloem connection in the
258 presence or absence of various concentrations of sucrose. (B) Expression profiles
259 for transcripts of a sugar-repressed gene (*GDH1*), and a sugar-induced gene
260 (*ApL3*) were plotted for intact, separated and grafted samples. (C)
261 Transcriptional overlap between previously published glucose-induced or
262 glucose repressed genes and our dataset. The number in brackets represents the
263 number of glucose-responsive genes identified in the previous dataset, and
264 overlap is presented as a ratio out of 1.0 for differentiation expressed genes
265 (DEG) up- or down-regulated in our dataset relative to intact samples. Asterisks
266 represent a significant difference ($p < 0.05$) between the ratio of up- and down-
267 regulated genes in a previously published transcriptome dataset compared to
268 the ratio of all up- and down- regulated genes in our grafting dataset at a certain
269 time point. (D) Lugol staining of grafted plants at various time points revealed
270 dark brown staining associated with starch accumulation. HAG, hours after
271 grafting.
272

273 **Table 1. Sugar response overlaps with asymmetry.** Symmetrically and
274 asymmetrically differentially expressed genes were compared to previously
275 published sugar-responsive genes (Osuna et al., 2007)[1] and the percent overlap
276 calculated (* p<.05). HAG, hours after grafting.
277

HAG	Sugar Induced[1]	Graft Bottom=Top	Overlap	%	Graft Top>Bottom	Overlap	%	Graft Bottom>Top	Overlap	%
6	2243	4988	263	5	6679	1403	21*	4971	99	2
12	2243	3473	165	5	7111	1444	20*	5657	231	4
24	2243	4135	171	4	6873	1414	21*	4942	195	4
48	2243	3689	197	5	6601	1241	19*	4915	218	4
72	2243	10421	1005	10*	2459	228	9*	2019	138	7
120	2243	15012	1063	7	1510	220	15*	941	115	12*
HAG	Sugar Repressed[1]	Graft Bottom=Top	Overlap	%	Graft Top>Bottom	Overlap	%	Graft Bottom>Top	Overlap	%
6	1998	4988	107	2	6679	53	1	4971	1563	31*
12	1998	3473	68	2	7111	112	2	5657	1526	27*
24	1998	4135	88	2	6873	72	1	4942	1525	31*
48	1998	3689	113	3	6601	93	1	4915	1427	29*
72	1998	10421	530	5	2459	111	5	2019	538	27*
120	1998	15012	979	7	1510	84	6	941	210	22*

278
279

280 **Vascular formation and cell division activates on both sides of the graft**

281 Since the grafted bottom samples exhibited a starvation response up to 48 hours
282 after grafting, we reasoned that pathways associated cell division and cell
283 differentiation would be delayed or inhibited. We looked at the expression of
284 markers associated with vascular formation and cell division in the
285 transcriptome datasets. Cambium, phloem and provascular markers activated
286 within 6 hours in grafted top samples, but activation was only delayed 6-24
287 hours in grafted bottom samples depending on the gene (Figure 1B-C, Figure 3,
288 Figure S5, Figure S6). Expression of phloem markers peaked in both grafted tops

289 and grafted bottoms at 72 hours (Figure 3, Figure S5, Figure S6), the time when
290 phloem reconnections form in grafted *Arabidopsis* (Figure 1, (Yin et al., 2012;
291 Melnyk et al., 2015)). Notably, the early phloem marker *NAC020* activated before
292 the mid phloem marker *NAC086* which activated before the late phloem marker
293 *NEN4*, consistent with the dynamics of phloem transcriptional activation during
294 primary root development and leaf vascular induction (Figure S5)(Furuta et al.,
295 2014; Kondo et al., 2016). Certain markers associated with xylem formation,
296 such as *VND7* and *BFN1*, activated early in the grafted top. Other xylem markers,
297 such as *IRX3* and *CESA4*, activated late in grafted samples. By 120 hours after
298 grafting, xylem markers were activated in top and bottom, consistent with when
299 the first xylem strands differentiate at the graft junction (Melnyk et al., 2015).
300 Genes associated with cell division were activated by 12 hours in the grafted top
301 and by 24 hours in the grafted bottom (Figure 3, Figure S5). On the other hand,
302 control genes whose expression does not typically vary between tissues and
303 treatments (Czechowski et al., 2005) were not differentially expressed in grafted
304 tops or bottoms (Figure S6). The RNAseq expression data appeared to correlate
305 well with transcriptional fluorescent reporters for both activation dynamics and
306 the localisation of expression (Figure 1D-F, Figure S2).
307
308 The similar activation dynamics of vascular differentiation genes in grafted tops
309 and grafted bottoms prompted us to test whether this phenomenon occurred
310 with other known developmental processes. We obtained lists of genes whose
311 expression is associated with various biological processes from previous
312 publications (Table S1) and tested how many of the genes differentially
313 expressed in our transcriptomes overlapped with the previously published lists.
314 Differentially expressed genes in grafted samples and separated tops partially
315 overlapped with those whose expression is associated with phloem, xylem and
316 procambium formation (Figure 4, Figure S7). There was a high overlap between
317 *Arabidopsis* inflorescence stem healing and grafting, as well as between vascular
318 induction in leaf disk cultures and grafting (Figure 4). Various genes expressed in
319 a cell type-specific manner also showed a high transcriptional overlap with
320 grafting, including phloem, endodermis and protoxylem (Figure 4, Figure S7). In
321 nearly all cases, the separated top, grafted top and grafted bottom samples

322 showed similar activation dynamics. The separated bottom samples were
323 exceptional though since gene expression associated with vascular development
324 and cell-specific processes was downregulated (Figure 4, Figure S7). We also
325 compared our datasets to RNAs expressed in longitudinal cross sections of the
326 *Arabidopsis* root (Brady et al., 2007). There was little overlap between grafted
327 bottoms and sections from the root meristemic zone, whereas overlap existed
328 between grafted tops and the root meristemic zone in early time points, and
329 between grafting and the root maturation zone (Figure S8). Our analysis also
330 revealed that two genes expressed in cambium, *WOX4* and *PXY*, were induced by
331 grafting but the primary root marker *WOX5* and lateral root marker *LBD18* were
332 not (Figure 3, Figure S5, Figure S6).

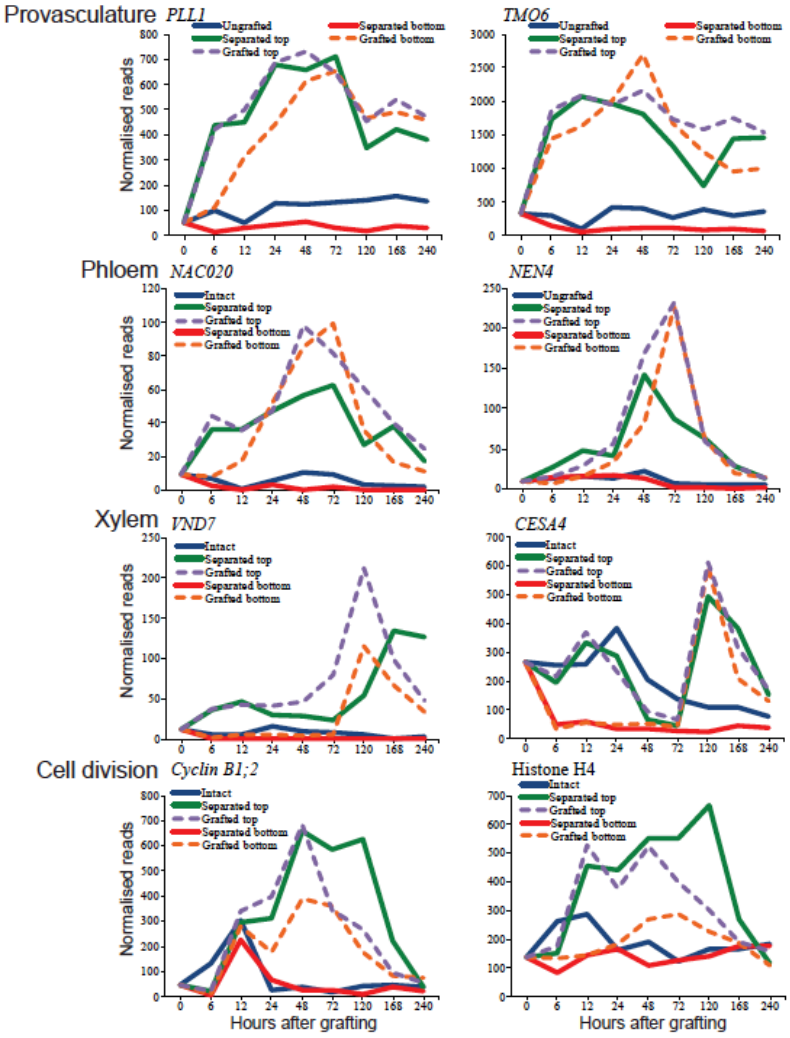

333

334 **Figure 3. Transcriptional dynamics of genes associated with**
335 **provasculature, phloem, xylem and cell division**. Expression levels were
336 plotted over time for intact, separated and grafted samples.
337

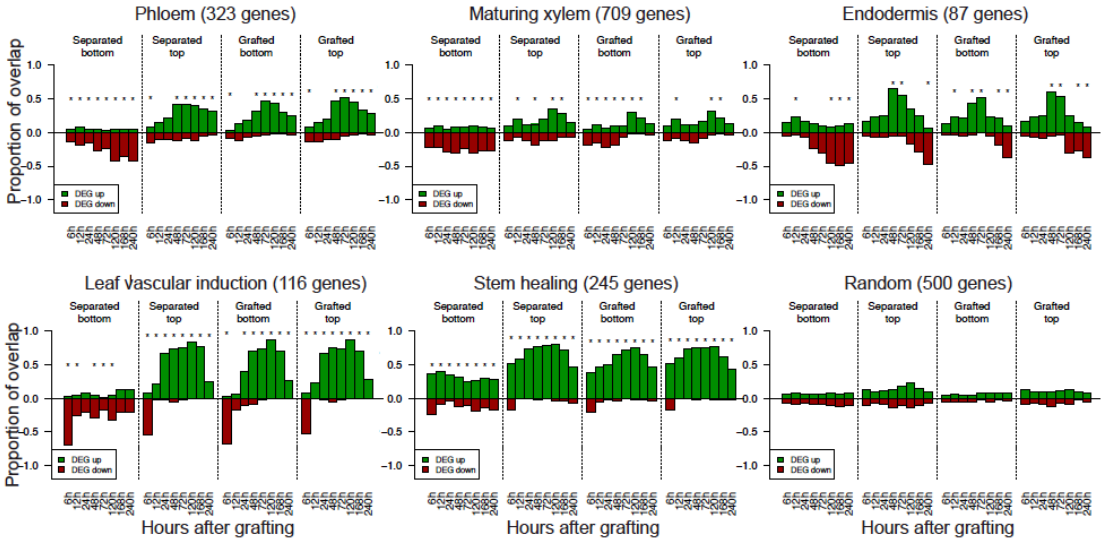

Figure 4. Transcriptional overlap between previously published vascular datasets and the grafting datasets. Genes whose transcripts are associated with various cell types or biological processes were taken from previously published datasets (see Table S1) and compared to the transcriptomic datasets generated here. The number in brackets represents the number of cell type-specific or process-specific genes identified in the previous dataset, and overlap is presented as a ratio out of 1.0 for differentiation expressed genes (DEG) up- or down-regulated in our dataset relative to intact samples. Asterisks represent a significant difference ($p < 0.05$) between the ratio of up- and down- regulated genes in a previously published transcriptome dataset compared to the ratio of all up- and down- regulated genes in our grafting dataset at a certain time point.

Auxin response is symmetric at the graft

The rapid activation of vascular markers in the grafted bottoms despite the starvation response promoted us to investigated whether other mobile substances such as phytohormones could play a role in gene activation. We compared lists of genes known to respond to cytokinin, ethylene or methyl jasmonate (Nemhauser et al., 2006) and found no substantial overlap between these lists and genes differentially expressed by grafting (Figure S9)(Table S1). Abscisic acid-responsive and brassinosteroid-responsive genes showed overlap with genes differentially expressed in our datasets, but this overlap was of a similar magnitude in both separated and grafted datasets suggesting the effect was not specific to grafting (Figure S9). Auxin responsive transcripts were exceptional though, as they showed a substantial overlap with RNAs differentially expressed in our data sets that varied depending on the treatment (Figure 5A-B, Figure S9). Auxin-induced genes were upregulated in separated tops, grafted bottoms and grafted tops whereas they were repressed in

366 separated bottoms (Figure 8). Auxin responsive genes such as *IAA1* and *IAA2*
367 (Abel et al., 1995) were induced to similar levels in grafted tops and grafted
368 bottoms at 24 hours. To further investigate whether auxin response was uniform
369 between grafted tops and grafted bottoms, we grafted the auxin-responsive
370 fluorescent reporter *p35S:DII-Venus* whose fluorescent protein is degraded in the
371 presence of auxin (Brunoud et al., 2012). DII-Venus fluoresced in the separated
372 bottoms but did not fluoresce in grafted bottoms 14 hours after cutting (Figure
373 5C) indicating separated bottoms had a low level of auxin response but grafted
374 tops, grafted bottoms and separated tops had a high level of auxin response.

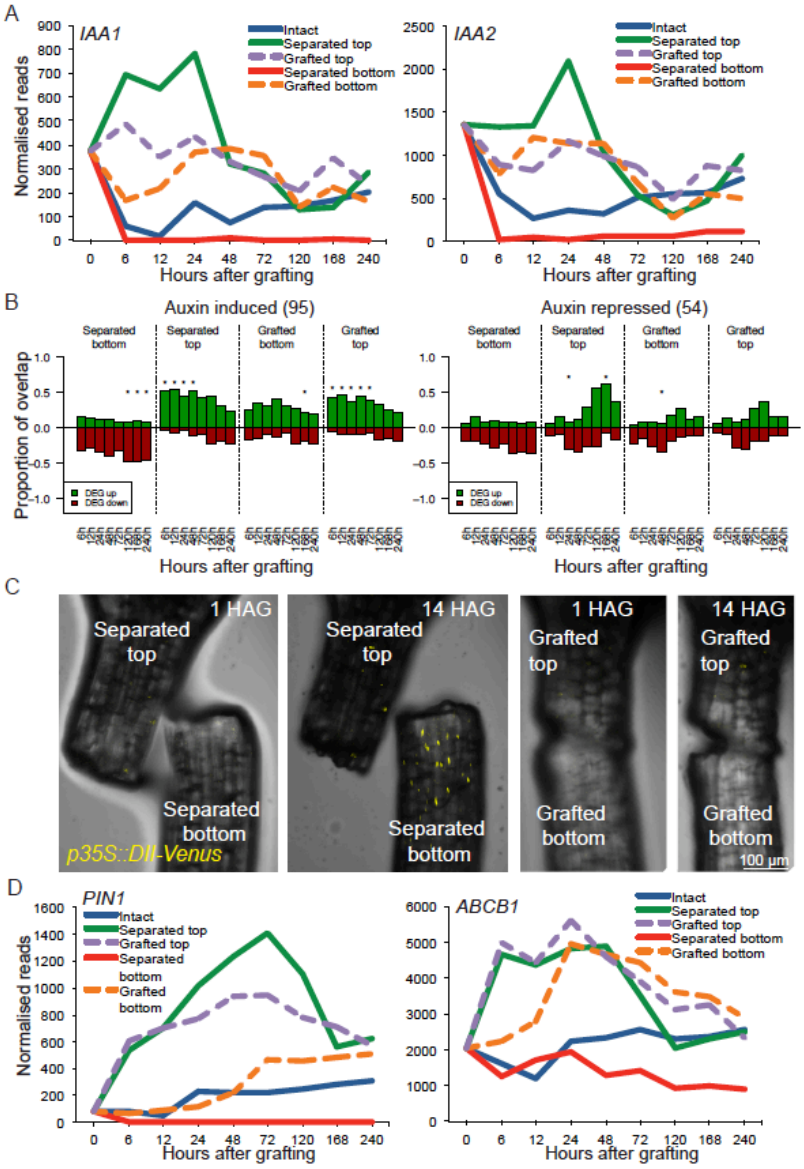

375

376 **Figure 5. Auxin response is symmetric at the graft junction.** (A,D) Expression
377 profiles for various auxin-responsive genes (*IAA1*, *IAA2*) or auxin transporter
378 genes (*PIN1* and *ABCB1* genes) were plotted for intact, separated and grafted
379 samples. (B) Overlap between previously published auxin-induced or auxin-

380 repressed RNAs and our dataset. The number in brackets represents the number
381 of auxin-responsive genes identified in the previous dataset, and overlap is
382 presented as a ratio out of 1.0 for differentiation expressed genes (DEG) up- or
383 down-regulated in our dataset relative to intact samples. Asterisks represent a
384 significant difference ($p < 0.05$) between the ratio of up- and down- regulated
385 genes in a previously published transcriptome dataset compared to the ratio of
386 all up- and down- regulated genes in our grafting dataset at a certain time point.
387 (C) Grafted and separated plants expressing the auxin responsive *p35S::DII-*
388 *Venus* transgene that is degraded in the presence of auxin reveal a reduction of
389 auxin response in cut bottoms, but not in grafted bottoms. HAG, hours after
390 grafting.
391

392 **Tissue fusion imparts a unique physiological response that differs from**
393 **tissue separation**

394 We hypothesized that the symmetric auxin response and asymmetric sugar
395 response at the graft junction could allow a unique transcriptional response
396 since neither separated plants nor intact plants had similar response dynamics
397 to sugars and auxin as measured by genome-wide gene response, starch
398 accumulation and *p35S::DII-Venus* expression (Figure 2, Figure 5). To uncover
399 protein-coding genes differentially expressed specifically by grafting, we
400 performed an empirical Bayesian analysis (Hardcastle & Kelly, 2010) where at
401 each time point we computed likelihoods for each gene for each possible pattern
402 of differential expression in the intact, grafted top, grafted bottom, separated top
403 and separated bottom tissues (Figure 6A). These likelihoods were used to define
404 a similarity score between pairs of genes, which was used to cluster genes with
405 similar patterns of gene expression across the five tissues (Hardcastle &
406 Papatheodorou, 2017). Clusters were then identified by the predominant pattern
407 of gene expression observed within a cluster. This analysis produced 113
408 clusters containing at least 10 RNAs at a single time point (Table S2; Dataset S1).
409 Approximately 6000 genes were differentially expressed in at least one tissue
410 whereas between 1000 and 4000 genes were not differentially expressed
411 (Figure 6B).
412

413 To simplify the analysis, we considered clusters where gene expression was
414 grouped into patterns consisting of one comparison. At early time points, the
415 cluster containing genes differentially expressed in grafted tops, grafted bottoms,

416 separated tops and separated bottoms had high numbers that decreased with
417 time and could represent an initial general wound response (Figure 6C).
418 Similarly, clusters containing separated tops and grafted tops or separated
419 bottoms and grafted bottoms initially had high numbers that decreased with
420 time. This observation indicated the grafted top was initially transcriptionally
421 similar to the separated top, whereas the grafted bottom was initially
422 transcriptionally similar to the separated bottom. After the 48-hour time point,
423 clusters containing genes only differentially expressed in separated tops or only
424 differentially expressed in separated bottoms increased in numbers, suggesting
425 these tissues gained a unique pattern of gene expression. The cluster containing
426 genes differentially expressed in grafted tops and grafted bottoms increase in
427 numbers throughout the healing process (Figure 6C). We searched for cluster
428 categories that contained genes only differentially expressed by grafting and
429 found very few genes downregulated by grafting or upregulated only in the
430 grafted top (Figure 7A). Instead, there were clusters that contained several
431 hundred differentially expressed genes present either in the grafted bottom only,
432 or present in both grafted bottom and grafted top (Figure 7A). Genes whose
433 expression changed only in the grafted bottom sample were prevalent early
434 during grafting and were most common at 48 hours, whereas genes activated in
435 both top and bottom became prevalent at 48 hours and were most common at
436 120 hours (Figure 7A). We performed a gene ontology (GO) analysis on the genes
437 whose expression was grafting-specific and found that genes coding for RNAs
438 differentially expressed only in the grafted bottom sample were enriched in the
439 immune response and chitin response biological process categories (Table S3).
440 Previously published chitin-induced RNAs had a high proportion of overlap with
441 differentially expressed graft bottom-specific genes (Figure 7E, Figure S10).
442 Grafting-specific RNAs expressed symmetrically, in both the grafted top and
443 grafted bottom, were enriched in vascular-related biological processes (Table
444 S3). Previously published phloem-enriched, endodermal-enriched, vascular-
445 induction and stem-wounding associated RNAs had a high proportion of overlap
446 with differentially expressed graft-specific genes (Figure 7C-D, Figure S10). Since
447 few genes were grafting-specific and grafted tissues were initially
448 transcriptionally quite similar to separated tissues (Figure 6C, Figure 7A), we

449 reasoned that tissues separated for short periods (<48 hours) could be grafted
450 with similar reconnection dynamics as tissues that had been grafted
451 immediately. To test this hypothesis, plants were cut at day 0, and grafted at 1-5
452 days after separation. Separated tissues did not speed up vascular reconnection,
453 and instead, it always took three days from the point of tissue attachment for
454 vascular connections to form (Figure S10). Furthermore, the shoot lost
455 competence to graft 2-3 days after separation whereas the root remained
456 competent to graft up to 5 days after separation (Figure S10). Together, it
457 appears the grafted shoot and root have a unique physiological response that
458 differ from separated plants and that tissue attachment is required to activate
459 graft formation and tissue fusion.

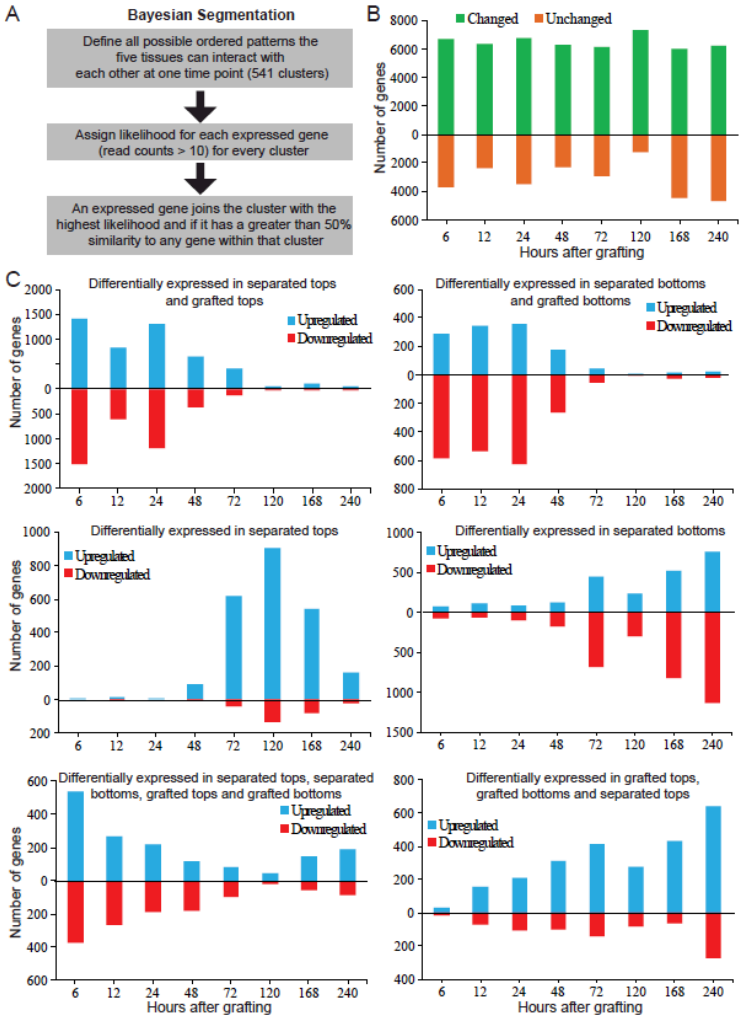

460

461 **Figure 6. Clustering the transcriptome at each time point, based on**
462 **likelihoods of all possible patterns of differential expression.** (A) Cartoon
463 depicting the Bayesian segmentation. (B) Analysis of differential behaviour
464 produced 113 categories containing at least 10 genes whose expression was
465 expressed in a specific differential pattern in at least one time point (see Table

S2). One group is comprised of genes whose transcript levels are not substantially changed in the five tissues (unchanged) whereas the other group is comprised of the sum of the other 112 groups (genes whose transcript levels changed after treatment in a least one tissue) over the time points tested. (C) Major categories in the segmentation revealed RNAs whose levels changed in all the treatments listed relative to intact samples. Note that a gene can be represented only in one category for a given time point, that category in which the transcript level changes best fit the category.

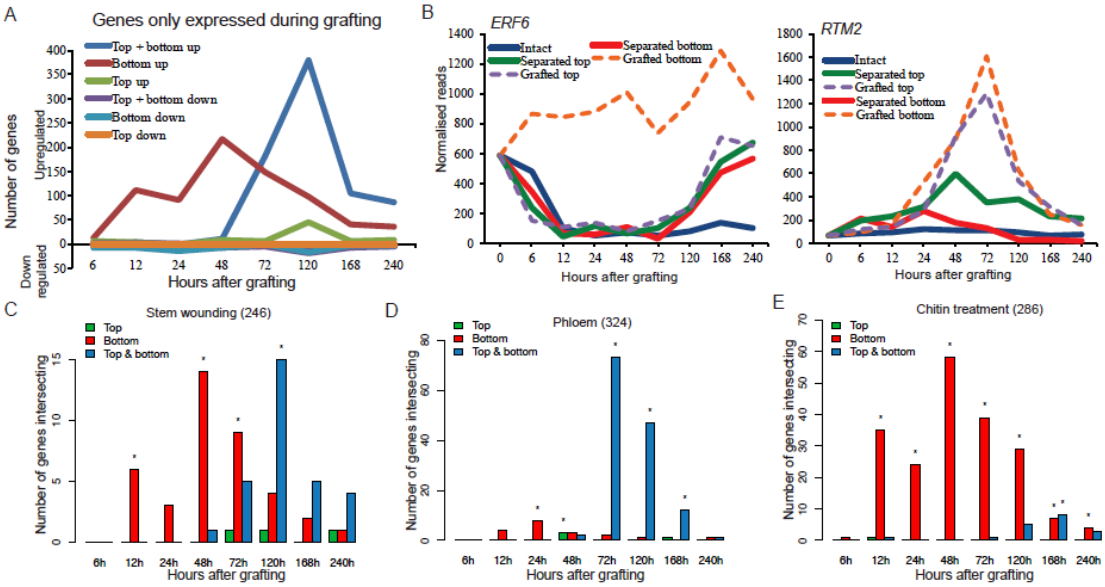

Figure 7. A subset of genes is differentially expressed only during graft formation when compared to 0 hour grafts, or intact or separated tissues. (A) Certain genes were only differentially expressed in grafted tops, grafted bottoms or both in grafted tops and grafted bottoms. (B) Expression profiles for a graft bottom-specific (*ERF6*) or a graft top and bottom differentially regulated gene (*RTM2*) were plotted for intact, separated and grafted samples. (C) Grafting-specific genes are also expressed in other processes of tissue fusion, such as stem healing. Here, 246 previously published RNAs whose differential expression is associated with stem healing were compared to our dataset to assess transcriptional overlap with the grafting-specific genes. Asterisks represent a significant high overlap ($p < 0.05$) of previously published genesets that are also differentially expressed in the grafted samples at a certain time point. (D-E) Genes differentially expressed in grafted tops and grafted bottoms show high overlap to 324 previously published genes whose transcripts are associated with phloem, whereas genes expressed in grafted bottoms show high overlap to 286 previously published genes whose encoded RNAs are associated with chitin treatment. Asterisks represent a significant high overlap ($p < 0.05$) of previously published genes that are also differentially expressed in the grafted samples at a certain time point.

498 **DISCUSSION**

499 To better understand how plants graft, we analysed in depth an RNA deep
500 sequencing dataset that spatially and temporally distinguished genes activated
501 by cutting and tissue attachment versus genes activated by cutting and
502 continuous tissue separation. We observed that during graft formation, tissues
503 had a very high transcriptional overlap with genes differentially expressed by
504 inflorescence stem healing and by vascular induction in leaves (Figure 4, Figure
505 S7) (Asahina et al., 2011; Kondo et al., 2016) suggesting grafting is closely related
506 to these processes. Graft formation had little transcriptional overlap with lateral
507 root formation (Figure S6)(Brady et al., 2007) and appeared to follow a pathway
508 similar to secondary root growth (Figure S6, Figure S8) since cambium-specific
509 markers *WOX4* and *PXY* were expressed during grafting and secondary growth
510 but are not expressed in the root tip (De Rybel et al., 2016)(Figure S5). Grafted
511 tops initially showed some transcriptional overlap with genes expressed during
512 primary root formation which may be related to the accumulation of substances
513 activating adventitious root formation, a common response in grafts that do not
514 properly form. However, this response was short lasting in grafted tops where
515 adjoining tissues could form vascular connections to re-establish substance
516 transport. Thus, we believe that grafting proceeds via a pathway involving
517 secondary growth with radial meristems activating in the mature cambium to
518 heal the wound. Vascular formation genes including those specifying cambium
519 and phloem were activated early, followed by an activation of cell division genes,
520 suggesting that the start of cellular differentiation preceded activation of cell
521 division. Xylem identity genes showed an early and a late activation peak (Figure
522 3, Figure S5). There is no visible xylem differentiation at the graft junction during
523 the first peak of expression (Melnyk et al., 2015) and these genes might be
524 suppressed by phloem differentiation genes such as *APL* and *CLE41* that activate
525 early after grafting and are known to suppress protoxylem formation (Bonke et
526 al., 2003; Ito et al., 2006)(Figure S6)(Table S4). Alternatively, the first peak could
527 represent programmed-cell death that does not lead to xylem differentiation.
528 The second expression peak of xylem-expressed genes at 120 hours occurred
529 after the differentiation of functional phloem and coincided with the
530 differentiation of xylem strands at the graft junction (Melnyk et al., 2015).

531 Previous studies highlighted the importance of callus and pericycle cells during
532 regeneration (Sugimoto et al., 2010; Iwase et al., 2011), but we see little evidence
533 that genes expressed in the pericycle or during callus formation have high
534 transcriptional overlap with genes differentially expressed by grafting (Figure
535 S4). Expression profiles for all protein-coding genes can be found in table S4.
536
537 We observe only a slight delay in phloem, cambium and cell division activation
538 below the graft junction compared to above it (Figure 3, Figure S5, Figure S6)
539 whereas some genes, such as *HCA2* and *TMO6,* activated equally in both grafted
540 top and grafted bottom at 6 hours after grafting (Figure 1D-G, Figure 3). These
541 data indicate that, at least transcriptionally, the grafted root rapidly responded
542 to the presence of the grafted shoot. This response was not present in separated
543 roots, indicating that attachment was key for recognition. Sugars are known
544 activators of cell division and cell elongation (Wang & Ruan, 2013) and in our
545 datasets, a large proportion of asymmetrically expressed genes are genes that
546 are sugar-responsive. However, sugars are transported in the phloem (Lough &
547 Lucas, 2006) that is severed upon grafting whereas the grafted root exhibited a
548 sugar starvation response and showed similar sugar-response dynamics as the
549 separated root. Instead, we believe that not sugar but auxin, or some other
550 molecular that is transported in the absence of vascular connections, could be
551 the signal in the grafted bottom that activates *HCA2*, *TMO6* as well as cell
552 division, phloem and cambium related genes.
553
554 Given auxin's role in vascular patterning and formation ((De Rybel et al., 2016), it
555 is a strong candidate for the activating signal. Auxin response was largely
556 symmetric, particularly from 12 hours after grafting (Figure 6) consistent with
557 previous findings that the auxin-inducible *DR5* and *ANAC071* genes are
558 symmetrically expressed around the graft junction (Yin et al., 2012;
559 Pitaksaringkarn et al., 2014; Melnyk et al., 2015; Matsuoka et al., 2016). One idea
560 is that auxin transport was not substantially interrupted by the grafting process,
561 and instead, where opposing tissues adhered, auxin moved regardless of
562 vascular connections since auxin is transported from cell to cell through the
563 apoplast (Leyser, 2011). The genes encoding auxin efflux proteins PIN1 and

564 ABCB1 were transcriptionally activated above the graft junction (Figure 5D),
565 similar to putative *Pisum sativum* PIN1 protein accumulating above a cut stem
566 prior to vascular reconnection (Sauer et al., 2006), and could reflect a role for
567 these proteins in exporting auxin across the cut. Consistent with these
568 observations, adding an auxin transport inhibitor to grafted *Arabidopsis* shoots
569 prevented the expression of grafting-induced genes below the graft junction
570 (Matsuoka et al., 2016). Since auxin is fundamental for patterning vasculature
571 (De Rybel et al., 2016), it is plausible that auxin movement across the graft
572 occurs prior to sugar movement since the flow of auxin could assist with
573 reconnecting the phloem. Although auxin response was symmetric, our previous
574 work demonstrated that the auxin response factors *ALF4* and *AXR1* affected
575 grafting only below the graft junction (Melnyk et al., 2015). Mutating *ALF4* below
576 the graft junction more strongly reduced auxin response than mutating *ALF4*
577 above the junction (Melnyk et al., 2015). Thus, proteins such as ALF4 or AXR1
578 might enhance or promote a rootstock-specific auxin response and could be
579 particularly important when there is incomplete attachment, cellular damage or
580 inefficient transport. All higher plants transport auxin from shoot to root, yet not
581 all plant species can be successfully grafted (Melnyk, 2017c) so the response to
582 auxin rather than the transport itself may be a determining factor in the ability to
583 graft. A role for sugars is not completely ruled out though, since the magnitude of
584 differential expression was often lower in the grafted bottom and exogenous
585 sugar reduced grafting efficiency (Figure 2A). Pericycle cells require auxin to
586 divide and the addition of sugars enhances the rate of divisions (Skylar et al.,
587 2011), suggesting that the presence of sugars in the grafted top enhanced cell
588 division and differentiation. Another hypothesis that warrants testing is whether
589 graft healing activates via a mechanical signal provided by the physical presence
590 of the opposing tissues.
591
592 Our analyses identified two groups of genes whose expression changes were
593 unique to graft formation in our experiments (Figure 7). One group activated
594 shortly after grafting below the graft junction and was enriched in immune-
595 responsive and chitin-responsive genes (Table S3, Figure 7, Figure S10). The
596 breakdown products of cell walls are potent elicitors of defence responses

597 (Souza et al., 2017), so it is possible that the grafted bottom upregulates
598 pathways specific to wound damage response. This group was not upregulated
599 in separated bottoms though, so the unique physiological state of the grafted
600 root, indicated by the presence of auxin response but the absence of sugar
601 response, could have promoted their upregulation. The second group activated
602 both above and below the graft junction and became highly expressed later
603 during graft formation (Figure 7). This group was enriched in RNAs associated
604 with vascular development (Table S3, Figure 7) and we suggest that the products
605 of these genes are involved in the vascular reconnection processes between the
606 two tissues. Despite many transcriptional similarities between separated tops
607 and grafted tissues, tissues had to be attached for at least three days for phloem
608 connections to form, regardless of when cutting occurred (Figure S10). Thus, it
609 appears that RNAs expressed in the separated top or separated bottom are
610 insufficient to drive graft formation. Instead attachment and the genes activated
611 by this recognition process including grafting-specific RNA changes (Figure 7A)
612 or RNAs expressed in the grafted bottom, grafted top and separated top (Figure
613 6C) are those that contribute to a response that distinguishes attached from
614 separated plant tissues. Future work should focus on these RNAs to identify the
615 pathways required for grafting that could be modified to improve graft
616 formation, wound healing and vascular regeneration. Likewise, the rapid
617 transcriptional changes below the graft indicate a recognition system that
618 promotes tissue regeneration. Identifying the exogenous cue that triggers
619 recognition and understanding how it is perceived should be priorities, as should
620 understanding whether this phenomenon applies more broadly to inter-tissue
621 communication, tissue regeneration or tissue fusion events, such as parasitic
622 plant infections (Musselman, 1980), epidermal fusions (Becraft et al., 1996; Lolle
623 et al., 1998) or petal fusions (Zhong & Preston, 2015).
624

625 **METHODS**

626 **Plant material and grafting**

627 *Arabidopsis thaliana* accession Columbia was used throughout. The *p35S::GFP-ER*
628 (Nelson et al., 2007), *pSUC2::GFP* (Imlau et al., 1999), *pUBQ10::PM-tdTomato*
629 (Segonzac et al., 2012), *pARR5::GFP* (Yanai et al., 2005), *pANT::H2B-YFP* (Randall

630 et al., 2015), *pLOG4::n3GFP* (De Rybel et al., 2014), *pCASP1::NLS-GFP* (Roppolo et
631 al., 2011), *p35S::DII-Venus* (Brunoud et al., 2012) lines have been previously
632 published. For the construction of *pHCA2::RFP*, a 2.9kb 5' upstream region of the
633 *HCA2* gene was cloned into pDONRp4-p1R donor vector, and recombined with
634 tagRFPer into a destination vector by the Multisite Gateway system (Siligato et
635 al., 2016). The following primers were used for *pHCA2* cloning: attB4_HCA2(-
636)2958 GGGACAACTTTGTATAGAAAAGTTGtcgatacgcgggacagatatac
637 attB1_HCA2ProEnd ggggACTGCTTTTTTGTACAAACTTGttttgtgttctgtatgtttg.
638 *Arabidopsis thaliana* micrografting was performed according to a previously
639 published protocol (Melnyk, 2017a). Briefly, seven day old *Arabidopsis* seedlings
640 were grown vertically on Murashige and Skoog (MS) medium + 1% bacto agar
641 (pH5.7; no sucrose) in short day conditions (8 hours of 80-100 µmol m^{-2} s^{-1} light)
642 at 20°C. Seedlings were placed on one layer of 2.5x4cm sterile Hybond N
643 membrane (GE Healthcare) on top of two 8.5cm circles of sterile 3 Chr Whatman
644 paper (Scientific Laboratory Supplies) moisten with sterile distilled water in a
645 9cm petri dish. In a laminar flow hood using a dissecting microscope, one
646 cotyledon was removed and a transvers cut through the hypocotyl was made
647 with a vascular dissecting knife (Ultra Fine Micro Knife; Fine Science Tools).
648 Grafts were assembled by aligning the two cut halves and joining them together,
649 after which, the petri dishes was sealed with parafilm and placed vertically
650 under short day conditions at 20°C. For grafting on a microscope coverslip to
651 image the graft junction, a 10cm square Petri dish modified by gluing a
652 microscope coverslip in place of a section of plastic from the back. On top of the
653 microscope cover slip was placed a 2.5x4 cm rectangle of Hybond N membrane.
654 At the edges and base of the Petri dish three 3 x 8cm strips of Whatman paper
655 were placed. Sterile water moistened both Whatman paper and Hybond N. After
656 which, roots were placed on the Hybond N membrane and hypocotyls on the
657 coverslip. Grafting then proceeded as above. Graft junctions were imaged
658 through the coverslip with a Plan-Apochromat 20X/0.8 objective on a Zeiss LSM-
659 700 or LSM-780 confocal microscope.
660
661 **Fluorescent assays and microscopy**

662 To test the effect of sugars on grafting, *Arabidopsis thaliana* Col-0 plants were
663 grown on 1/2MS+ 1% bacto agar (pH5.7; no sucrose) for seven days in short day
664 conditions. Wild type roots were grafted to scions expressing *pSUC2::GFP* using
665 the protocol described above but either water or water containing 0.25%, 0.5%
666 1% or 2% sucrose was added to the grafted plates. Roots were observed for
667 fluorescence 2-7 days after grafting with a Zeiss V12 dissecting microscope
668 equipped with a GFP filter. Roots were scored daily and the same plants were
669 observed during the 7-day assay as previously described (Melnyk, 2017b).
670
671 Fluorescent images were taken on a Zeiss LSM-700 or LSM-780 confocal
672 microscope with a Zeiss Plan-Apochromat 20X/0.8 dry objective. A 488nm argon
673 laser (Zeiss 780) or 488nm solid-state laser (Zeiss 700) was used for excitation
674 of GFP and YFP. A 561nm solid-state laser was used for excitation of the
675 tdTomato fluorescent protein. A T-PMT detector obtained bright-field
676 transmitted light. Black and white fluorescent images of graft junctions were
677 taken on a Zeiss V12 dissecting microscope fitted with a Hamamatsu EM-CCD
678 camera and RFP and YFP filters. FIJI software (Fiji.sc) was used to process
679 images. Image contrast and brightness were adjusted for controls and samples
680 equally. For longitudinal images of the graft junction, z-stack projections are
681 shown and made with the average intensity function in FIJI from stacks
682 containing the hypocotyl vascular tissues, mesophyll and epidermis.
683
684 **RNAseq sample and library preparation**
685 Wild type *Arabidopsis thaliana* accession Col-0 were grafted as above taking care
686 to switch shoot and root between different plants. All grafting and cutting was
687 performed in the morning to minimize circadian effects. For the 0 hour time
688 points, plants were transferred from 1/2MS plates to the grafting plates and
689 immediately harvested. Only intact plants were harvested at the 0 hour time
690 since at this point, there would be insufficient time to reasonably expect the
691 separated or grafted samples to be transcriptionally different (the time between
692 cutting and freezing is less than two minutes). For all other time points, after
693 cutting plants were left on grafting plates for the respective amount of time.
694 Tissues were harvested and care taken to separate grafts by gently pulling plants

695 apart. Approximately 0.5mm of tissue was taken above or below each cut site
696 and kept separate. Intact plants had 1mm of tissue taken in a similar location on
697 the hypocotyl as separated or grafted plants. Grafted, separated or intact tissues
698 were pooled into groups of approximately 24 tissues (1 plates with 24 plants)
699 which were immediately placed in 96% ethanol on dry ice. After harvesting,
700 microcentrifuge tubes were briefly centrifuged and the ethanol removed before
701 storing at -80°C. Plants were grafted over two months to get sufficient material.
702
703 Tissues were ground in the microcentrifuge tube using a microcentrifuge pestle
704 frozen in liquid nitrogen. RNA was extracted using an RNeasy Kit (Qiagen, UK)
705 following the manufacturer's instructions including on column DNase digestion.
706 RNA was eluted from the column with 50ul of sterile water. Quality and quantity
707 of RNA was checked using an Agilent 2200 TapeStation and High Sensitivity (HS)
708 RNA screentapes (Agilent, UK). After RNA extraction, two to four biological
709 replicates were combined (50-100 plants) to get sufficient RNA. 90-100ng of
710 RNA was used to prepare RNAseq libraries using the TruSeq® Stranded mRNA
711 LT kit (Illumina, UK) according to the manufacturer's instructions. The final PCR
712 was for 15 cycles and samples were resuspended in 23ul of distilled water.
713 Quantity and quality of DNA libraries was checked on the Agilent 2200
714 TapeStation using D1000 screentapes (Agilent, UK). Each sample had two
715 libraries prepared from grafted tissues or separated tissues at different times so
716 that independent biological replicates were made. Samples were diluted to 10nM
717 and 11-12 barcoded samples randomly mixed to make a total of 7 mixes for 7
718 flow lanes, one mix per lane. Samples were sequenced on the HiSeq 4000
719 platform (Illumina, UK) with Paired End 75bp transcriptome sequencing (BGI
720 Tech Solutions, Shenzhen, China).
721
722 **Iodine staining**
723 *Arabidopsis* seedlings were placed in a fixation solution (3.7% formaldehyde,
724 50% ethanol, 5% acetic acid) for 1 hour at room temperature, then transferred
725 to 70% ethanol for 10 minutes. Afterwards, plants were transferred to 96%
726 ethanol and stored at -20°C for up to a week. Samples were rehydrated in 50%
727 ethanol for 1 hour at room temperature, then transferred to distilled water for

728 30 minutes. Samples were then transferred to a solution of Lugol solution
729 (Sigma) and stained for 10 minutes at room temperature. Plants were rinsed
730 with water, then mounted on microscope slides. Images were taken on a Zeiss
731 Axioimager.M2 microscope with a PlanApochromat 20x objective and SPOT Flex
732 camera (Imsol, UK).
733
734 **Pairwise and Bayseq analyses**
735 The reads acquired through high-throughput sequencing were quality trimmed
736 with sickle (Joshi & Fass, 2011) to increase the read quality before mapping.
737 Reads were aligned to protein-coding gene sequences acquired from TAIR10
738 using Bowtie2. Read assignment was performed using the eXpress tool, which
739 also provided effective gene lengths for use in normalisation. Library scaling
740 factors were inferred from the sum of the number of reads assigned to the genes
741 in the lowest seventy-five percentiles of expressed genes for each library
742 (Hardcastle et al., 2012).
743
744 Analyses of the data were carried out using the R package baySeq (Hardcastle &
745 Kelly, 2010)and clustering based on the posterior probabilities acquired from
746 this package. For each timepoint, all possible patterns of differential expression
747 between the graft types were considered, where a 'pattern' defines similarity and
748 difference between different experimental conditions. For example,
749 *'{Col_cut_bottomGenes=Col:Col_bottomGenes=ungraftedGenes},{Col_cut_topGenes=Col:Col_topGenes}'*
750 defines a pattern in which gene expression is equivalent in the separated
751 bottoms, the grafted bottoms and the intact plant, but different to the
752 equivalently expressed separated top and grafted top. The total number of
753 possible patterns for five experimental conditions (as in this analysis) is fifty-
754 two.
755
756 For a given timepoint, posterior likelihoods on the likelihood of each pattern of
757 expression are calculated for every gene with greater than ten reads across all
758 experimental conditions. The patterns were then modified to include orderings
759 (denoted by < or >), for example, the pattern described would lead to the
760 ordered pattern

761 *'{Col_cut_bottomGenes=Col:Col_bottomGenes=ungraftedGenes}>{Col_cut_topGenes=Col:Col_topGenes}'*
762 in which gene expression is equivalent in the separated bottoms, the grafted
763 bottoms and the intact plant and greater than the equivalently expressed
764 separated top and grafted top. In total, 541 ordered patterns exist in this data
765 set. Posterior likelihoods for an ordered pattern were assigned to that of the
766 unordered pattern for genes in which the (normalised) mean expressions within
767 the equivalently expressed groups conformed to the ordering, and to zero
768 otherwise.
769
770 Based on the posterior likelihoods for the ordered patterns, a similarity score s_{ij}
771 was established between two genes *i* and *j* as the sum over the products of their
772 likelihoods of each ordered pattern. A single-link agglomerative clustering of
773 genes, in which a gene will join a cluster if it has a greater than 50% similarity to
774 any gene within that cluster was then performed based on these similarity
775 scores. We label each cluster according to the predominant ordered pattern with
776 high likelihood amongst the genes that comprise it. The change in size of these
777 clusters over time is shown for the major clusterings in Figure 6.
778
779 We can also find likelihoods on comparisons between pairs of experimental
780 conditions by summing the likelihoods over combinations of patterns. Figure 1B
781 shows the number of genes identified at each time point in a pairwise analysis
782 between the grafted top and grafted bottom samples. The likelihood of
783 symmetric expression (i.e., expression which is equivalent across the graft
784 junction) is calculated as the sum of the likelihoods of all patterns in which the
785 grafted top and grafted bottom samples are equivalent. Conversely, asymmetric
786 expression is calculated as the sum of the likelihoods of all patterns in which the
787 grafted top and grafted bottom samples are not equivalent. Additional sets can
788 be formed by considering the ordering of the grafted top and grafted bottoms
789 samples. Sets of genes are identified at each time point with an FDR of less than
790 0.05 and a likelihood of symmetric/asymmetric expression greater than 50%.
791 Genes in this analysis were only included if they were differentially expressed
792 relative to intact samples.
793

794 **Gene overlap analyses of up and down regulated genes**

795 To measure if the ratio of up- and down- regulated genes from a previously
796 published dataset is significantly different to the ratio of up- and down-regulated
797 genes in our grafting dataset we only took into account genes that are
798 differentially expressed at a certain time point. A gene was called differentially
799 expressed at a certain time point if the marginal likelihood, calculated by BaySeq,
800 was greater than 0.9 and if the absolute $\log_2$-foldchange was greater than 1.
801 Hence, we only consider genes that are significantly two-fold up- or down-
802 regulated. This definition of differentially expressed genes was also used to filter
803 the published datasets according to the expression values in our transcriptome
804 dataset. Hence, some genes were filtered out from the original published
805 datasets because they did not show a significant up- or down- regulation during
806 a certain time point in our expression data based on our criteria. The histograms
807 (Figure 2,4, 5, S4, S7, S8, S9) show the relative number of up- and down-
808 regulated genes from the published datasets during a certain time point and a
809 certain condition (separated top, separated bottom, grafted top, grafted bottom)
810 based on the number of genes in the published dataset after filtering. To
811 calculate the significance of the difference of the ratios between the published
812 DEGs and all up- and down- regulated genes, we used a two-sided Fisher's exact
813 test. To correct for multiple testing we used the Benjamini-Yekutieli (BY)
814 correction method. Hence, the asterisks in the barplots highlight that the
815 corrected p-value is below 0.05.

816

817 **Dealing with probe ids from microarray datasets**

818 Due to the fact that some published datasets only used probe ids instead of gene
819 ids to represent their differentially expressed genes we first had to match these
820 probe ids to their corresponding gene ids. This step was done with the R package
821 biomartr (Drost & Paszkowski, 2017). If one probe id matched more than one
822 gene id we used all the corresponding gene ids and tested afterwards if these
823 genes were actually differentially expressed in our dataset. In some cases, one
824 probe id was represented by more than one gene id. Hence, some gene sets
825 contained slightly more gene ids than published probe ids. In contrast, some

826 probe ids did not match to currently existing gene ids. Hence, some gene sets
827 contained slightly fewer gene ids than published probe ids.
828
829 **Gene overlap analyses of gene sets involved in graft formation**
830 For this analysis we used the previously calculated gene sets from `baySeq` of
831 differentially expressed genes clustered for each time point into grafted bottom,
832 grafted top, and grafted bottom and top and calculated their overlap to
833 previously published data sets. The significance of the number of overlapping
834 genes between the grafted samples and the published datasets was determined
835 by a one-sided Fisher's exact test, to prove if the overlap is greater than
836 expected. The resulting p-values were corrected for multiple testing by using the
837 Benjamini-Yekutieli method.
838 This procedure was also applied to generate Table 1 to study the overlaps of
839 symmetrically and asymmetrically expressed genes in the grafting dataset with
840 previously published sugar-responsive genes.
841
842 **GO enrichment analysis**
843 The gene ontology analysis (GO) enrichment analysis on grafting-specific genes
844 was done with a customized R script using the package GOstats (Falcon &
845 Gentleman, 2007). Gene ontology annotation was used from the Bioconductor
846 package org.At.tair.db (Carlson, 2017). The p-values calculated by a
847 hypergeometric test were corrected for multiple testing with the Bonferroni
848 correction. A GO category was called enriched if the corrected p-value was below
849 0.05.
850
851 A detailed description, the required data and R scripts to reproduce the
852 clustering (hierarchical clustering and PCA), the statistical analyses regarding
853 the overlap studies, and the GO enrichment analysis are available via the GitHub
854 repository (https://github.com/AlexGa/GraftingScripts).
855
856 **Breaking force measurements**
857 A micro-extensometer was used for all breaking force graft measurements
858 according to a previously published protocol (Robinson et al., 2017). Briefly,

859 grafted Col-0 plants were attached to a moving plate using tough tags (0.94X0.50
860 inches, white, 679 catalog no. TTSW-1000, DiversifiedBiotech) and a
861 cyanoacrylate glue. The plates were moved apart and the force was measured
862 using a force sensor (Futek LSB200 10g load cell, Futek Inc.). Upon breaking the
863 force dropped. The maximum force measured before breaking was recorded.
864 Images were captured using a Leica SP5 confocal microscope. During the
865 experiment single z-place images were captured and made into a movie in
866 ImageJ.
867
868 To measure levels of tissue contamination between grafted top and bottom,
869 grafted green fluorescent protein(*p35S::GFP*) and red fluorescent protein
870 (*pUBQ10::PM-tdTomato*) expressing plants were pulled apart manually and
871 imaged on a Zeiss LSM 700 confocal microscope. Z-stacks comprising the
872 majority of the hypocotyl were made and regions approximately 0.5mm above
873 and 0.5mm below the graft junction were made into projections using the
874 average intensity function on FIJI software, and then the mean intensity
875 quantified for red and green channels on FIJI. The mean intensity of one colour in
876 the tissue tested for contamination was divided by the mean intensity of the
877 same colour in the tissue expressing that transgenes to get a percentage of
878 contamination. A region away from the cut site was also quantified to get a
879 percentage of spectral overlap between red and green channels. The percent
880 spectral overlap was then subtracted from the percentage contamination to get
881 an overall percentage for how much contamination was present.
882
883 **ACKNOWLEDGEMENTS**
884 We thank Niko Geldner, Dolf Weijers, Paul Tarr, Yka Helariutta, Ruth Stadler and
885 The Arabidopsis Information Resource for providing seeds. Funding for this
886 work was provided by Gatsby Charitable Trust grants GAT3272/C and GAT3273-
887 PR1, by a Knut and Alice Wallenberg Academy Fellowship KAW2016.0274 (to
888 C.W.M), and by the Howard Hughes Medical Institute and Gordon and Betty
889 Moore Foundation grant GBMF3406 (to E.M.M.)
890
891

892 **REFERENCES**

893 **Abel S, Nguyen MD, Theologis A. (1995).** The PS-IAA4/5-like family of early
894 auxin-inducible mRNAs in Arabidopsis thaliana. *J Mol Biol* **251**(4): 533-
895 549.
896 **Aloni R. (1980).** Role of auxin and sucrose in the differentiation of sieve and
897 tracheary elements in plant tissue cultures. *Planta* **150**(3): 255-263.
898 **Asahina M, Azuma K, Pitaksaringkarn W, Yamazaki T, Mitsuda N, Ohme-**
899 **Takagi M, Yamaguchi S, Kamiya Y, Okada K, Nishimura T, et al.**
900 **(2011).** Spatially selective hormonal control of RAP2.6L and ANAC071
901 transcription factors involved in tissue reunion in Arabidopsis.
902 *Proceedings of the National Academy of Sciences of the United States of*
903 *America* **108**(38): 16128-16132.
904 **Becraft PW, Stinard PS, McCarty DR. (1996).** CRINKLY4: A TNFR-like receptor
905 kinase involved in maize epidermal differentiation. *Science* **273**(5280):
906 1406-1409.
907 **Bonke M, Thitamadee S, Mahonen AP, Hauser MT, Helariutta Y. (2003).** APL
908 regulates vascular tissue identity in Arabidopsis. *Nature* **426**(6963): 181-
909 186.
910 **Brady SM, Orlando DA, Lee JY, Wang JY, Koch J, Dinneny JR, Mace D, Ohler U,**
911 **Benfey PN. (2007).** A high-resolution root spatiotemporal map reveals
912 dominant expression patterns. *Science* **318**(5851): 801-806.
913 **Brunoud G, Wells DM, Oliva M, Larrieu A, Mirabet V, Burrow AH, Beeckman**
914 **T, Kepinski S, Traas J, Bennett MJ, et al. (2012).** A novel sensor to map
915 auxin response and distribution at high spatio-temporal resolution.
916 *Nature* **482**(7383): 103-106.
917 **Carlson M 2017**. org.At.tair.db: Genome wide annotation for Arabidopsis.
918 **Chen Z, Zhao J, Hu F, Qin Y, Wang X, Hu G. (2017).** Transcriptome changes
919 between compatible and incompatible graft combination of Litchi
920 chinensis by digital gene expression profile. *Scientific reports* **7**(1): 3954.
921 **Cheong YH, Chang HS, Gupta R, Wang X, Zhu T, Luan S. (2002).**
922 Transcriptional profiling reveals novel interactions between wounding,
923 pathogen, abiotic stress, and hormonal responses in Arabidopsis. *Plant*
924 *physiology* **129**(2): 661-677.
925 **Chitwood DH, Guo M, Nogueira FT, Timmermans MC. (2007).** Establishing
926 leaf polarity: the role of small RNAs and positional signals in the shoot
927 apex. *Development* **134**(5): 813-823.
928 **Cookson SJ, Clemente Moreno MJ, Hevin C, Nyamba Mendome LZ, Delrot S,**
929 **Magnin N, Trossat-Magnin C, Ollat N. (2014).** Heterografting with
930 nonself rootstocks induces genes involved in stress responses at the graft
931 interface when compared with autografted controls. *Journal of*
932 *experimental botany* **65**(9): 2473-2481.
933 **Cookson SJ, Clemente Moreno MJ, Hevin C, Nyamba Mendome LZ, Delrot S,**
934 **Trossat-Magnin C, Ollat N. (2013).** Graft union formation in grapevine
935 induces transcriptional changes related to cell wall modification,
936 wounding, hormone signalling, and secondary metabolism. *Journal of*
937 *experimental botany* **64**(10): 2997-3008.
938 **Cordoba E, Aceves-Zamudio DL, Hernandez-Bernal AF, Ramos-Vega M, Leon**
939 **P. (2015).** Sugar regulation of SUGAR TRANSPORTER PROTEIN 1 (STP1)

940 expression in Arabidopsis thaliana. *Journal of experimental botany* **66**(1):
941 147-159.
942 **Czechowski T, Stitt M, Altmann T, Udvardi MK, Scheible WR. (2005).**
943 Genome-wide identification and testing of superior reference genes for
944 transcript normalization in Arabidopsis. *Plant physiology* **139**(1): 5-17.
945 **De Rybel B, Adibi M, Breda AS, Wendrich JR, Smit ME, Novak O, Yamaguchi**
946 **N, Yoshida S, Van Isterdael G, Palovaara J, et al. (2014).** Plant
947 development. Integration of growth and patterning during vascular tissue
948 formation in Arabidopsis. *Science* **345**(6197): 1255215.
949 **De Rybel B, Mahonen AP, Helariutta Y, Weijers D. (2016).** Plant vascular
950 development: from early specification to differentiation. *Nat Rev Mol Cell*
951 *Biol* **17**(1): 30-40.
952 **Drost HG, Paszkowski J. (2017).** Biomartr: genomic data retrieval with R.
953 *Bioinformatics* **33**(8): 1216-1217.
954 **Falcon S, Gentleman R. (2007).** Using GOstats to test gene lists for GO term
955 association. *Bioinformatics* **23**(2): 257-258.
956 **Furuta KM, Yadav SR, Lehesranta S, Belevich I, Miyashima S, Heo JO, Vaten**
957 **A, Lindgren O, De Rybel B, Van Isterdael G, et al. (2014).** Plant
958 development. Arabidopsis NAC45/86 direct sieve element morphogenesis
959 culminating in enucleation. *Science* **345**(6199): 933-937.
960 **Goldschmidt EE. (2014).** Plant grafting: new mechanisms, evolutionary
961 implications. *Frontiers in plant science* **5**: 727.
962 **Hardcastle TJ, Kelly KA. (2010).** baySeq: empirical Bayesian methods for
963 identifying differential expression in sequence count data. *BMC*
964 *Bioinformatics* **11**: 422.
965 **Hardcastle TJ, Kelly KA, Baulcombe DC. (2012).** Identifying small interfering
966 RNA loci from high-throughput sequencing data. *Bioinformatics* **28**(4):
967 457-463.
968 **Hardcastle TJ, Papatheodorou I. (2017).** clusterSeq: methods for identifying
969 co-expression in high-throughput sequencing data. *bioRxiv* **188581**.
970 **Ikeuchi M, Iwase A, Rymen B, Lambolez A, Kojima M, Takebayashi Y,**
971 **Heyman J, Watanabe S, Seo M, De Veylder L, et al. (2017).** Wounding
972 triggers callus formation via dynamic hormonal and transcriptional
973 changes. *Plant physiology*.
974 **Imlau A, Truernit E, Sauer N. (1999).** Cell-to-cell and long-distance trafficking
975 of the green fluorescent protein in the phloem and symplastic unloading
976 of the protein into sink tissues. *The Plant cell* **11**(3): 309-322.
977 **Ito Y, Nakanomyo I, Motose H, Iwamoto K, Sawa S, Dohmae N, Fukuda H.**
978 **(2006).** Dodeca-CLE peptides as suppressors of plant stem cell
979 differentiation. *Science* **313**(5788): 842-845.
980 **Iwase A, Mitsuda N, Koyama T, Hiratsu K, Kojima M, Arai T, Inoue Y, Seki M,**
981 **Sakakibara H, Sugimoto K, et al. (2011).** The AP2/ERF transcription
982 factor WIND1 controls cell dedifferentiation in Arabidopsis. *Current*
983 *Biology* **21**(6): 508-514.
984 **Joshi NA, Fass JN 2011**. Sickle: A sliding-window, adaptive, quality-based
985 trimming tool for FastQ files (Version 1.33).
986 **Kondo Y, Nurani AM, Saito C, Ichihashi Y, Saito M, Yamazaki K, Mitsuda N,**
987 **Ohme-Takagi M, Fukuda H. (2016).** Vascular Cell Induction Culture
988 System Using Arabidopsis Leaves (VISUAL) Reveals the Sequential

989 Differentiation of Sieve Element-Like Cells. *The Plant cell* **28**(6): 1250-
990 1262.
991 **Lee J, Kubota C, Tsao SJ, Bie Z, Echevarria PH, Morra L, Oda M. (2010).**
992 Current status of vegetable grafting: Diffusion, grafting techniques,
993 automation. *Scientia Horticulturae* **127**: 93-105.
994 **Leyser O. (2011).** Auxin, self-organisation, and the colonial nature of plants.
995 *Current Biology* **21**(9): R331-337.
996 **Lindsay DW, Yeoman MM, Brown R. (1974).** An analysis of the development of
997 the graft union in Lycopersicon esculentum. *Annals of Botany* **38**: 639-
998 646.
999 **Lolle SJ, Hsu W, Pruitt RE. (1998).** Genetic analysis of organ fusion in
1000 Arabidopsis thaliana. *Genetics* **149**(2): 607-619.
1001 **Lough TJ, Lucas WJ. (2006).** Integrative plant biology: Role of phloem long-
1002 distance macromolecular trafficking. *Annual review of plant biology* **57**:
1003 203-232.
1004 **Marsch-Martinez N, Franken J, Gonzalez-Aguilera KL, de Folter S, Angenent**
1005 **G, Alvarez-Buylla ER. (2013).** An efficient flat-surface collar-free
1006 grafting method for Arabidopsis thaliana seedlings. *Plant methods* **9**(1):
1007 14.
1008 **Matsumoto-Kitano M, Kusumoto T, Tarkowski P, Kinoshita-Tsujimura K,**
1009 **Vaclavikova K, Miyawaki K, Kakimoto T. (2008).** Cytokinins are
1010 central regulators of cambial activity. *Proceedings of the National Academy*
1011 *of Sciences of the United States of America* **105**(50): 20027-20031.
1012 **Matsuoka K, Sugawara E, Aoki R, Takuma K, Terao-Morita M, Satoh S,**
1013 **Asahina M. (2016).** Differential Cellular Control by Cotyledon-Derived
1014 Phytohormones Involved in Graft Reunion of Arabidopsis Hypocotyls.
1015 *Plant & cell physiology* **57**(12): 2620-2631.
1016 **Melnyk CW. (2017a).** Grafting with Arabidopsis thaliana. *Methods in molecular*
1017 *biology* **1497**: 9-18.
1018 **Melnyk CW. (2017b).** Monitoring Vascular Regeneration and Xylem
1019 Connectivity in Arabidopsis thaliana. *Methods in molecular biology* **1544**:
1020 91-102.
1021 **Melnyk CW. (2017c).** Plant grafting: insights into tissue regeneration.
1022 *Regeneration* **4**(1): 3-14.
1023 **Melnyk CW, Schuster C, Leyser O, Meyerowitz EM. (2015).** A developmental
1024 framework for graft formation and vascular reconnection in Arabidopsis
1025 thaliana. *Current Biology* **25**(10): 1306-1318.
1026 **Moore R. (1984).** Graft formation in Solanum pennellii (Solanaceae). *Plant Cell*
1027 *Reports* **3**(5): 172-175.
1028 **Musselman LJ. (1980).** The biology of Striga, Orobanche, and other root-
1029 parasitic weeds. *Annual Review of Phytopathology* **18**: 463-489.
1030 **Nelson BK, Cai X, Nebenfuhr A. (2007).** A multicolored set of in vivo organelle
1031 markers for co-localization studies in Arabidopsis and other plants. *The*
1032 *Plant Journal* **51**(6): 1126-1136.
1033 **Nemhauser JL, Hong F, Chory J. (2006).** Different plant hormones regulate
1034 similar processes through largely nonoverlapping transcriptional
1035 responses. *Cell* **126**(3): 467-475.
1036 **Osuna D, Usadel B, Morcuende R, Gibon Y, Blasing OE, Hohne M, Gunter M,**
1037 **Kamlage B, Trethewey R, Scheible WR, et al. (2007).** Temporal

1038 responses of transcripts, enzyme activities and metabolites after adding
1039 sucrose to carbon-deprived Arabidopsis seedlings. *The Plant journal : for*
1040 *cell and molecular biology* **49**(3): 463-491.
1041 **Pitaksaringkarn W, Ishiguro S, Asahina M, Satoh S. (2014).** ARF6 and ARF8
1042 contribute to tissue reunion in incised Arabidopsis inflorescence stems.
1043 *Plant Biotechnology* **31**(1): 49-53.
1044 **Randall RS, Miyashima S, Blomster T, Zhang J, Elo A, Karlberg A, Immanen J,**
1045 **Nieminen K, Lee JY, Kakimoto T, et al. (2015).** AINTEGUMENTA and
1046 the D-type cyclin CYCD3;1 regulate root secondary growth and respond to
1047 cytokinins. *Biology open*.
1048 **Robinson S, Huflejt M, Barbier de Reuille P, Braybrook SA, Schorderet M,**
1049 **Reinhardt D, Kuhlemeier C. (2017).** An automated confocal micro-
1050 extensometer enables in vivo quantification of mechanical properties
1051 with cellular resolution. *bioRxiv* **183533**.
1052 **Roppolo D, De Rybel B, Tendon VD, Pfister A, Alassimone J, Vermeer JE,**
1053 **Yamazaki M, Stierhof YD, Beeckman T, Geldner N. (2011).** A novel
1054 protein family mediates Casparian strip formation in the endodermis.
1055 *Nature* **473**(7347): 380-383.
1056 **Sauer M, Balla J, Luschnig C, Wisniewska J, Reinohl V, Friml J, Benkova E.**
1057 **(2006).** Canalization of auxin flow by Aux/IAA-ARF-dependent feedback
1058 regulation of PIN polarity. *Genes & development* **20**(20): 2902-2911.
1059 **Segonzac C, Nimchuk ZL, Beck M, Tarr PT, Robatzek S, Meyerowitz EM,**
1060 **Zipfel C. (2012).** The shoot apical meristem regulatory peptide CLV3
1061 does not activate innate immunity. *The Plant cell* **24**(8): 3186-3192.
1062 **Siligato R, Wang X, Yadav SR, Lehesranta S, Ma G, Ursache R, Sevilem I,**
1063 **Zhang J, Gorte M, Prasad K, et al. (2016).** MultiSite Gateway-Compatible
1064 Cell Type-Specific Gene-Inducible System for Plants. *Plant physiology*
1065 **170**(2): 627-641.
1066 **Skylar A, Sung F, Hong F, Chory J, Wu X. (2011).** Metabolic sugar signal
1067 promotes Arabidopsis meristematic proliferation via G2. *Dev Biol* **351**(1):
1068 82-89.
1069 **Souza CA, Li S, Lin AZ, Boutrot F, Grossmann G, Zipfel C, Somerville SC.**
1070 **(2017).** Cellulose-Derived Oligomers Act as Damage-Associated
1071 Molecular Patterns and Trigger Defense-Like Responses. *Plant physiology*
1072 **173**(4): 2383-2398.
1073 **Sugimoto K, Jiao Y, Meyerowitz EM. (2010).** Arabidopsis regeneration from
1074 multiple tissues occurs via a root development pathway. *Developmental*
1075 *cell* **18**(3): 463-471.
1076 **Thum KE, Shin MJ, Palenchar PM, Kouranov A, Coruzzi GM. (2004).** Genome-
1077 wide investigation of light and carbon signaling interactions in
1078 Arabidopsis. *Genome biology* **5**(2): R10.
1079 **Villadsen D, Smith SM. (2004).** Identification of more than 200 glucose-
1080 responsive Arabidopsis genes none of which responds to 3-O-
1081 methylglucose or 6-deoxyglucose. *Plant molecular biology* **55**(4): 467-
1082 477.
1083 **Wang L, Ruan YL. (2013).** Regulation of cell division and expansion by sugar
1084 and auxin signaling. *Frontiers in plant science* **4**: 163.
1085 **Wetmore RH, Rier JP. (1963).** Experimental induction of vascular tissues in
1086 callus of angiosperms. *American Journal of Botany* **50**(5): 418-430.

1087 **Yanai O, Shani E, Dolezal K, Tarkowski P, Sablowski R, Sandberg G, Samach**
1088 **A, Ori N. (2005).** Arabidopsis KNOXI proteins activate cytokinin
1089 biosynthesis. *Current Biology* **15**(17): 1566-1571.
1090 **Yin H, Yan B, Sun J, Jia P, Zhang Z, Yan X, Chai J, Ren Z, Zheng G, Liu H.**
1091 **(2012).** Graft-union development: a delicate process that involves cell-
1092 cell communication between scion and stock for local auxin accumulation.
1093 *Journal of experimental botany* **63**(11): 4219-4232.
1094 **Zheng BS, Chu HL, Jin SH, Huang YJ, Wang ZJ, Chen M, Huang JQ. (2010).**
1095 cDNA-AFLP analysis of gene expression in hickory (Carya cathayensis)
1096 during graft process. *Tree physiology* **30**(2): 297-303.
1097 **Zhong J, Preston JC. (2015).** Bridging the gaps: evolution and development of
1098 perianth fusion. *New Phytologist* **208**(2): 330-335.
1099
1100
1101
1102
1103
1104
1105
1106
1107
1108
1109
1110
1111
1112
1113
1114
1115
1116
1117
1118
1119
1120
1121
1122
1123
1124

1125 **SUPPLEMENTARY MATERIAL**

1126 **Movie S1. Breaking weight measurements at the graft junction, related to**
1127 **figure 1.** A micro-extensometer pulled apart an Arabidopsis plant 9 days after
1128 grafting while force was measured using a force sensor and images captured
1129 using a Zeiss Sp5 confocal microscope. Here, the transmitted light field is shown.
1130 Shoot is on top and root towards the bottom.
1131
1132 **Movie S2. Breaking weight measurements at the graft junction, related to**
1133 **figure 1.** A micro-extensometer pulled apart an *Arabidopsis* plant 9 days after
1134 grafting while force was measured using a force sensor and images captured
1135 using a Zeiss Sp5 confocal microscope. The same experiment is shown in Movie
1136 S1, but here, the GFP and RFP channels are shown. Shoot is on top (*p35S::GFP*
1137 expressing) and root towards the bottom (*pUBQ10::PM-tdTomato* expressing).
1138
1139 **Table S1.** Details of previously published datasets used to compare to the
1140 grafting datasets.
1141
1142 **Table S2.** Numbers and categories associated with the Bayseq analysis.
1143 Categories are defined as grafted (Col:Col), separated (Col_cut) or intact
1144 (ungrafted).
1145
1146 **Table S3.** GO analysis for biological process (BP). Shown are the top 20 BP GO
1147 terms for the grafting-specific genes. Time point selected are those when there
1148 are the most genes in grafted bottom samples (48hrs) or grafted top + bottom
1149 samples (120 hrs).
1150
1151 **Table S4.** Normalised reads for all the protein-coding genes in the datasets. By
1152 entering the ATG number of interest, a plot is made which shows a differential
1153 gene expression profile for the gene of interest.
1154
1155 **Dataset S1.** Details of the Bayesian segmentation analysis providing files
1156 containing the ATGs for every cluster for every time point.
1157

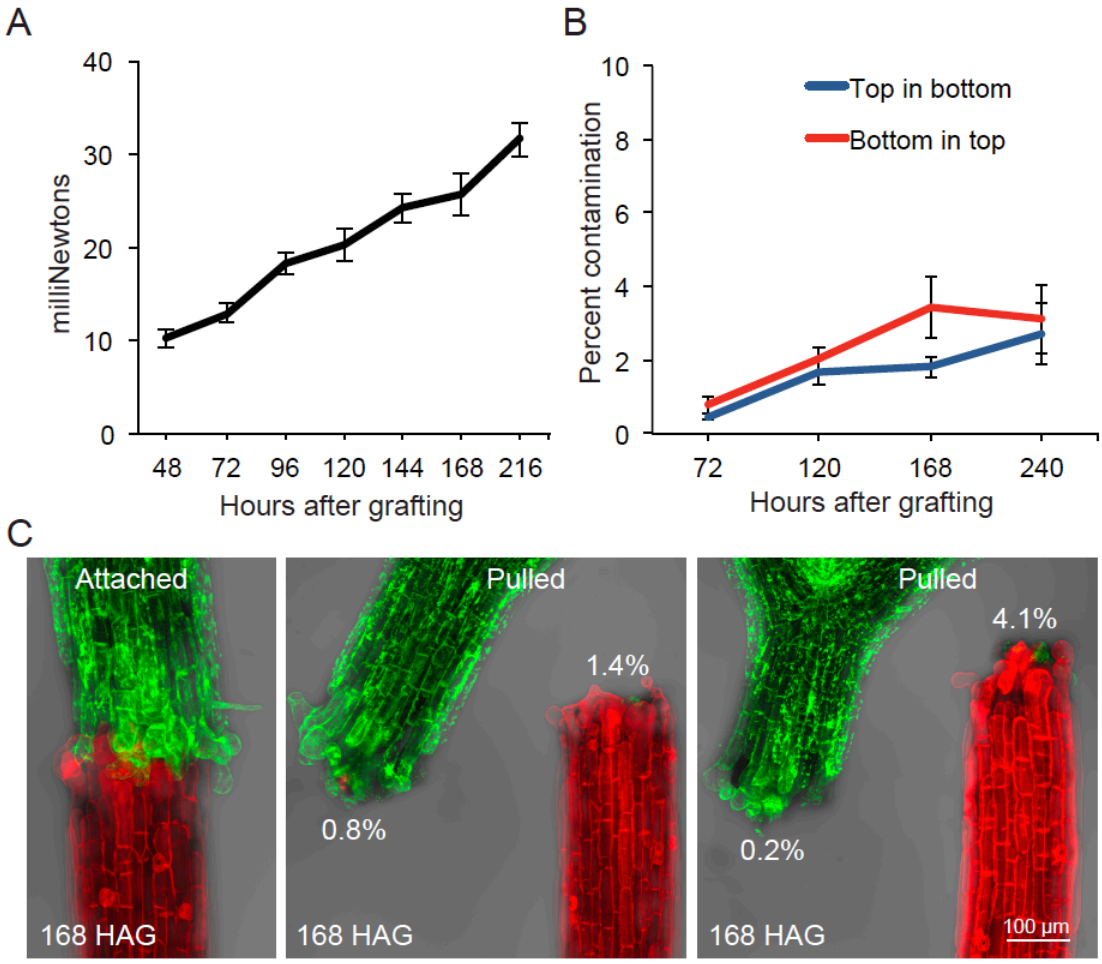

Figure S1. Experimental approach, related to figure 1. (A) The breaking weight required to pull apart grafted plants measured by a micro-extensometer. (B-C) Contamination of top in bottom or bottom in top was less than 4% as measured by grafting green fluorescent protein-expressing plants (*p35S::GFP*) to tomato fluorescent protein-expressing plants (*pUBQ10::PM-tdTomato*) and measuring amounts of fluorescence at the different wavelengths of emission in the top segments relative to the bottom. Images show different plants prior to and after pulling with the percent contamination indicated.

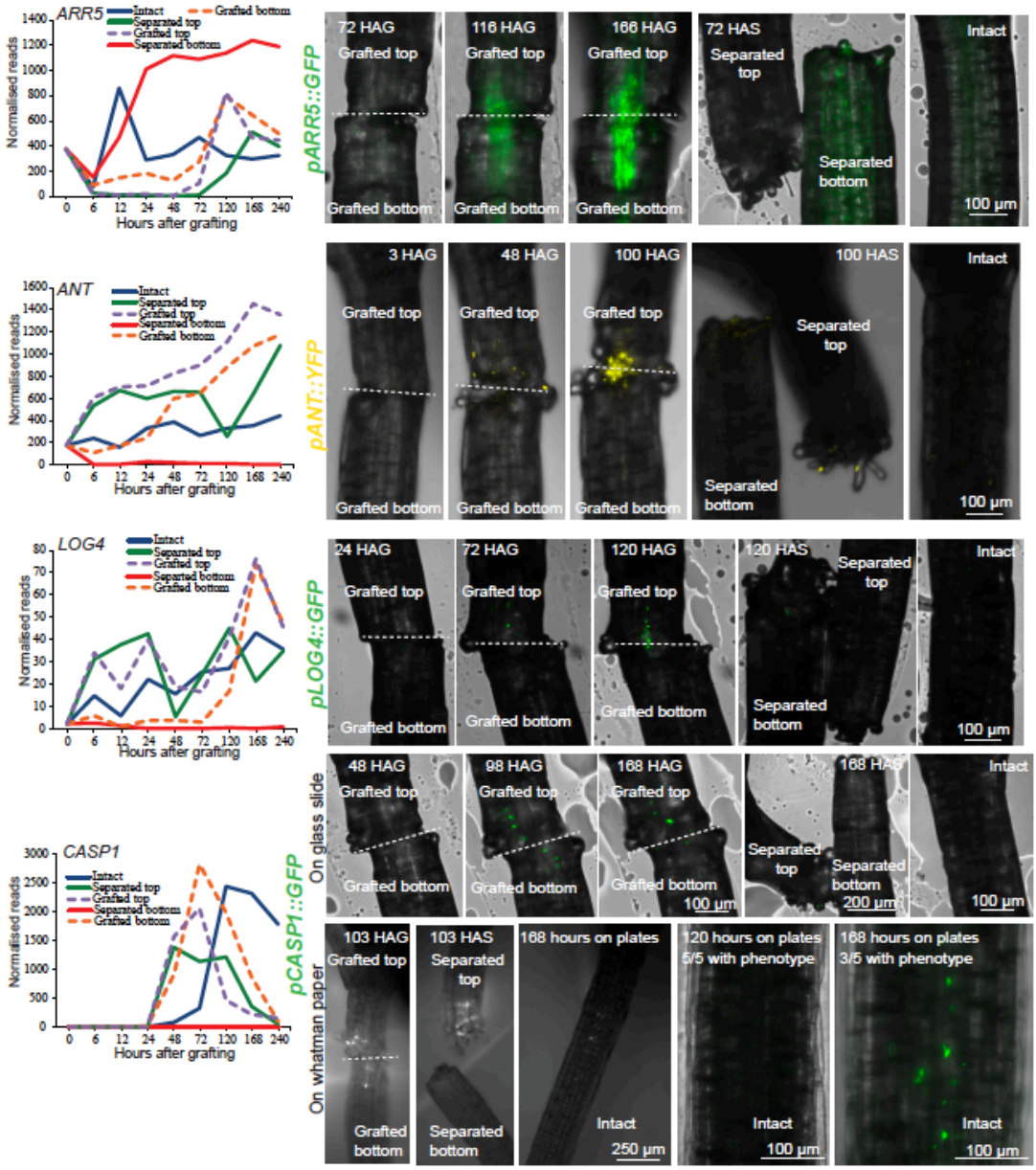

Figure S2. Comparison between RNAseq transcriptome expression profiles and transcriptional fluorescent reporters, related to figure 1. RNAseq expression profiles for various genes upregulated during graft formation were plotted for intact, separated and grafted samples (left panels). Transcriptional reporter-expressing plants were cut and separated, cut and grafted, or left intact. After cutting, plants were imaged and z-projections made at various time points (right panels). For *pCASP1::GFP*, we did not observe a signal in intact plants grafted on glass slides (see Materials and Methods), but observed a signal with 3/5 plants 7 days after grafting on Whatman-nylon membrane, the same condition used for transcriptome library preparation. HAG, hours after grafting. HAS, hours after separation. Dashed lines denote the graft junction.

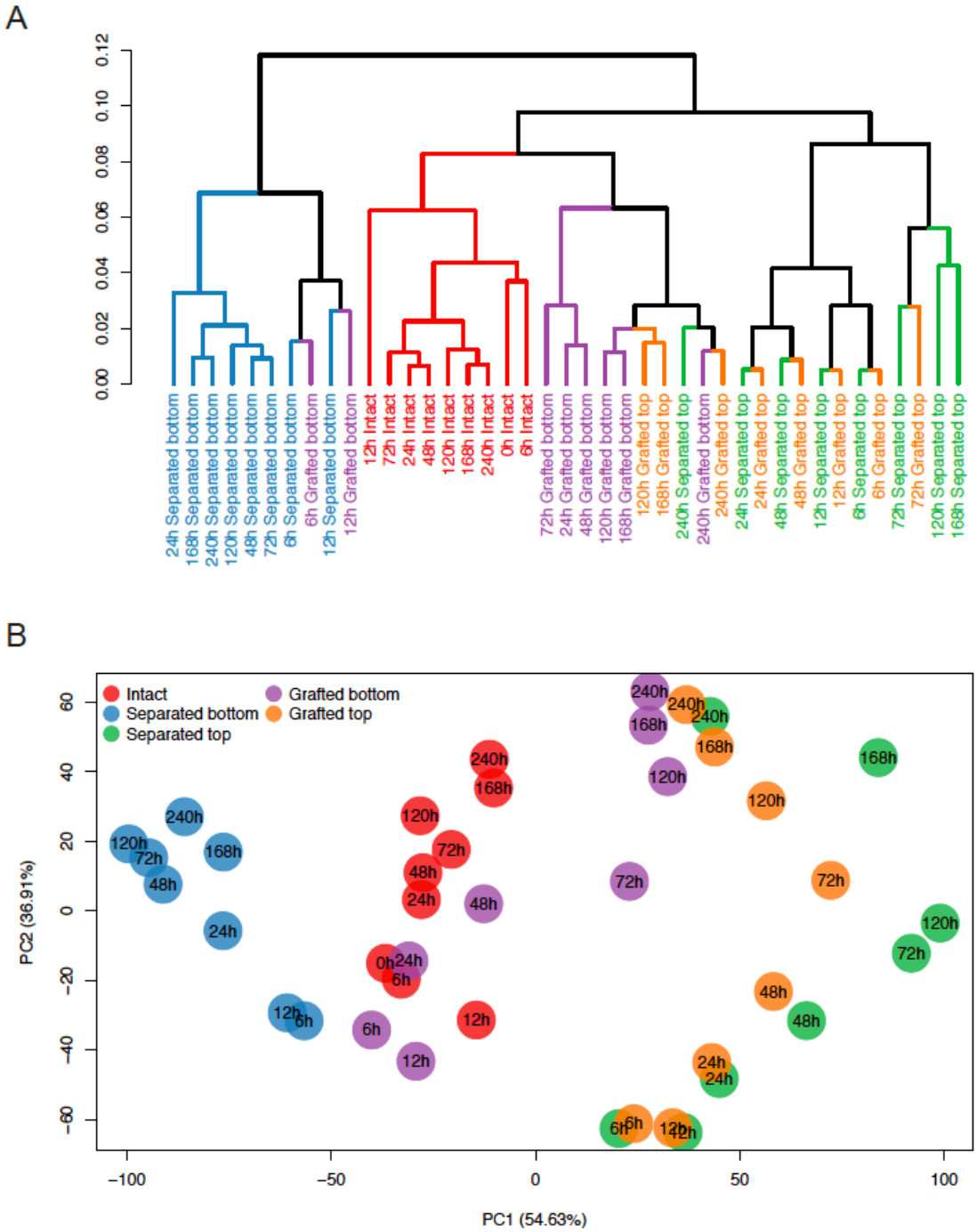

Figure S3. Hierarchical cluster analysis and principle component analysis (PCA) for the transcriptome libraries, related to figure 1. (A) Hierarchical clustering of samples based on log10 transformed TPM values. Similarity between samples was measured by 1 – spearman correlation coefficient. (B) PCA of expression data shows clustering of similar samples. Especially the grafted top and grafted bottom samples are very similar from 120 hours onwards.

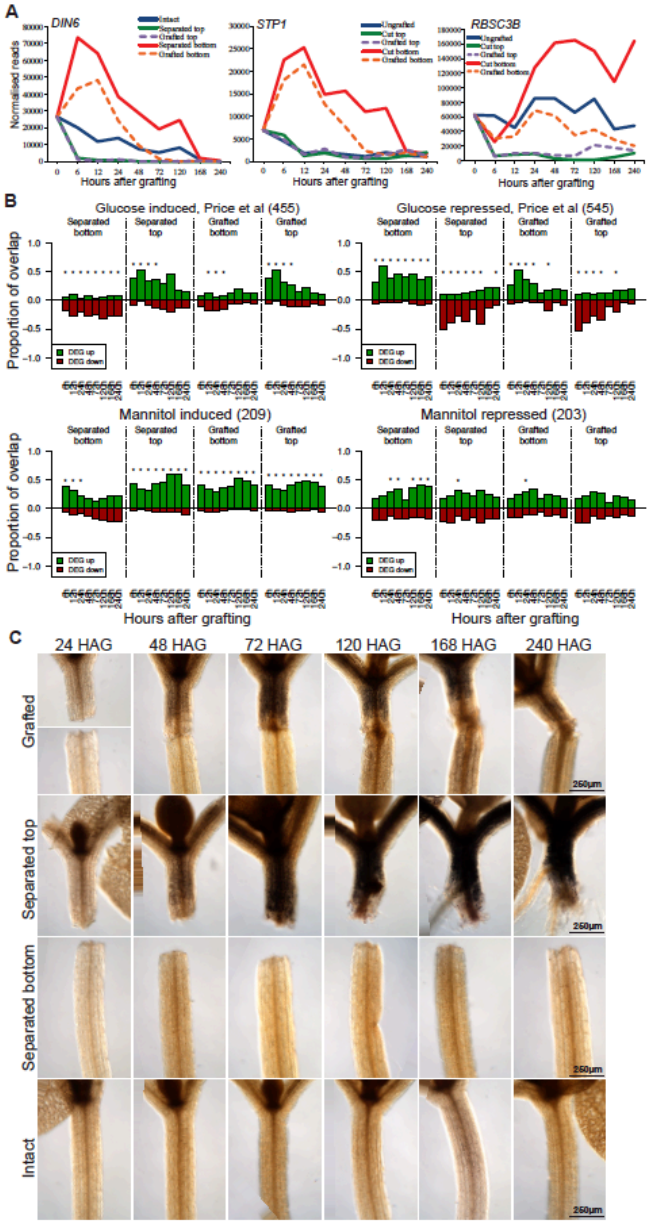

Figure S4. Asymmetry is a feature observed with sugar response and starch accumulation, related to figure 2. (A) Expression profiles for RNAs coded by sugar-repressed genes (*DIN6*, *STP1*) or photosynthetic gene (*RBSC3B*) were plotted for intact, separated and grafted samples. (B) Transcriptional overlap between previously published mannitol-induced, mannitol-repressed, sugar-induced or sugar-repressed genes and our datasets. The numbers in brackets represents the number of glucose or mannitol-responsive genes identified in the previous dataset, and overlap is presented as a ratio out of 1.0 for differentially expressed genes (DEG) up or down regulated in our dataset relative to intact samples. Asterisks represent a significant difference ($p < 0.05$) between the ratio of up- and down- regulated genes in a previously published transcriptome dataset compared to the ratio of all up- and down- regulated genes in our grafting dataset at a certain time point. (C) Lugol staining of grafted plants at various time points reveals dark brown staining associated with starch accumulation. Upper grafted panels are the same as those present in Figure 2 and shown here to compare with controls. HAG, hours after grafting.

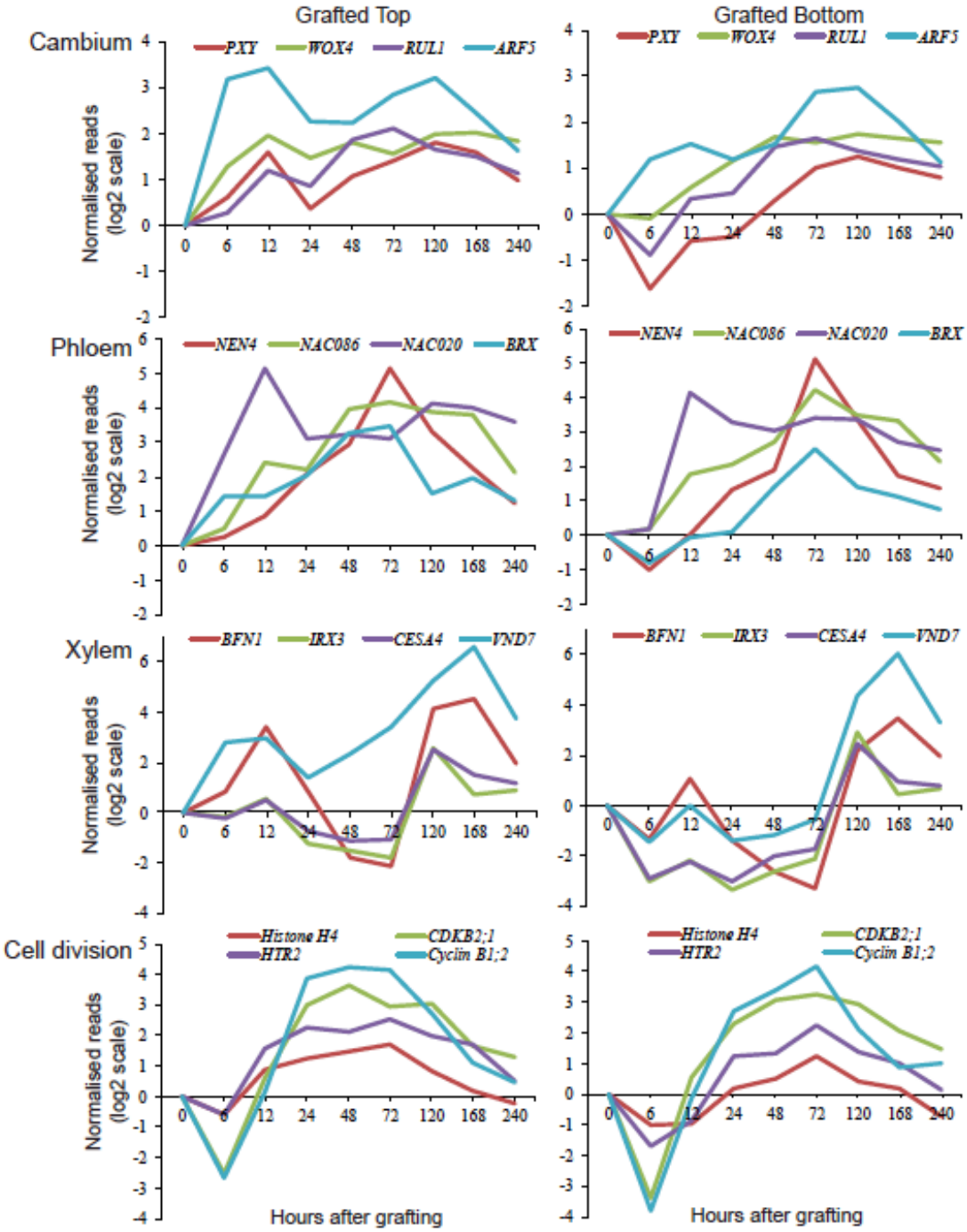

Figure S5. Transcriptional dynamics of genes associated with cambium, phloem, xylem and cell division, related to figure 3. Expression profiles in grafted tops or grafted bottoms for various genes of interest were plotted, normalised to intact samples and plotted on a $\log_2$ scale.

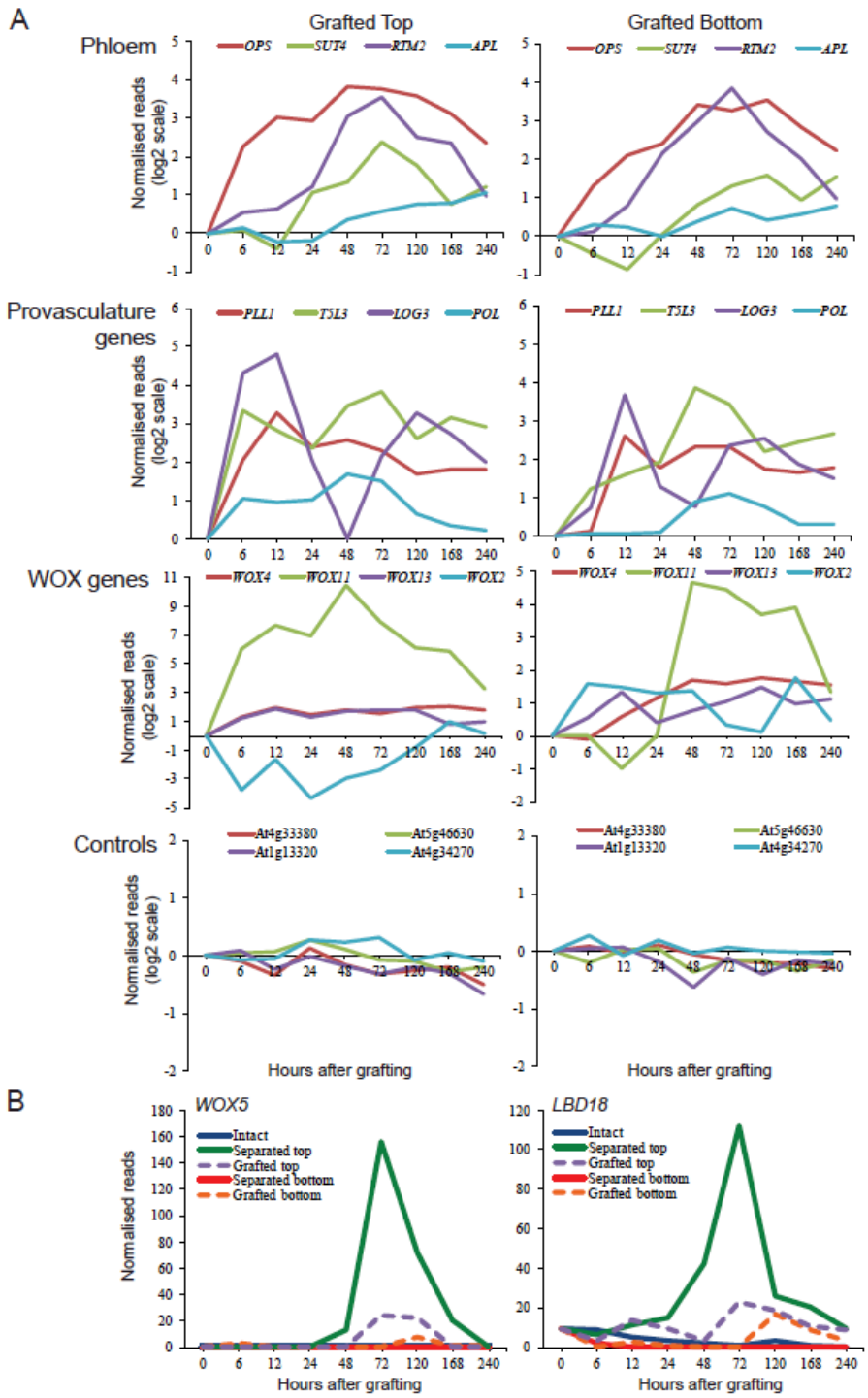

Figure S6. Accumulation of RNA from genes associated with provasculature and phloem, and of RNAs from WOX transcription factors, related to figure 3. (A) RNA accumulation profiles for various genes of interest were plotted over time as measured in grafted tops or grafted bottoms, normalised to intact samples and plotted on a $\log_2$ scale. The grafting datasets could also be used to investigate the transcriptional dynamics of related genes, such as the sequential activation of WOX transcription factors at the graft junction. (B) Expression levels of a primary root specific transcript (of the *WOX5* gene) or a lateral root specific transcript (from the *LBD18* gene) were plotted over time for intact, separated and grafted samples.

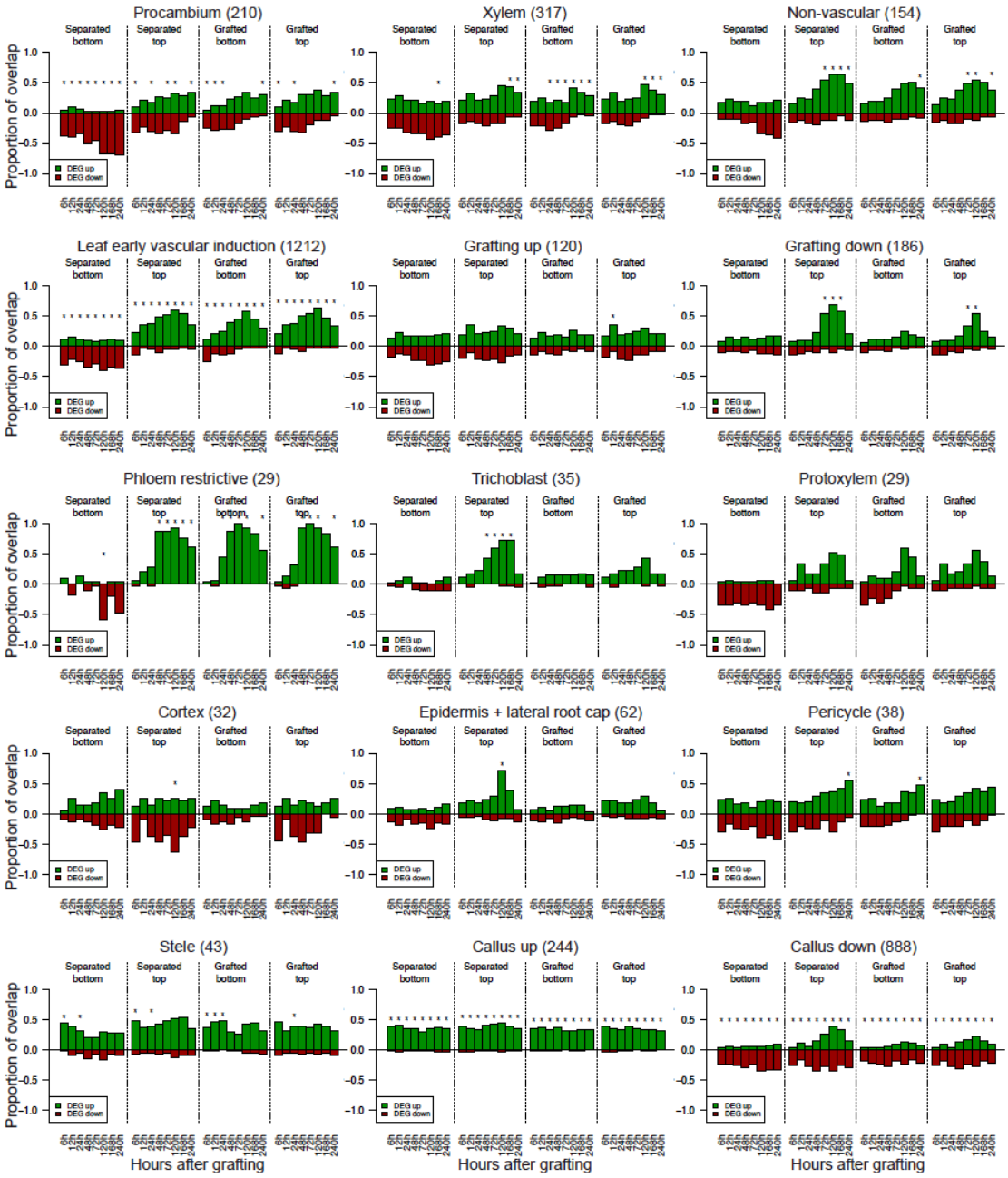

Figure S7. Transcriptional overlap between previously published datasets and the grafting datasets, related to Figure 4. Genes whose transcripts are associated with various cell types or biological processes were taken from previously published datasets (see Table S1) and compared to the datasets generated here. The number in brackets represents the number of cell type-specific or process-specific genes identified in the previous dataset, and overlap is presented as a ratio out of 1.0 for differentiation expressed genes (DEG) up- or down-regulated in our dataset relative to intact samples. Asterisks represent a significant difference ($p < 0.05$) between the ratio of up- and down- regulated genes in a previously published transcriptome dataset compared to the ratio of all up- and down- regulated genes in our grafting dataset at a certain time point.

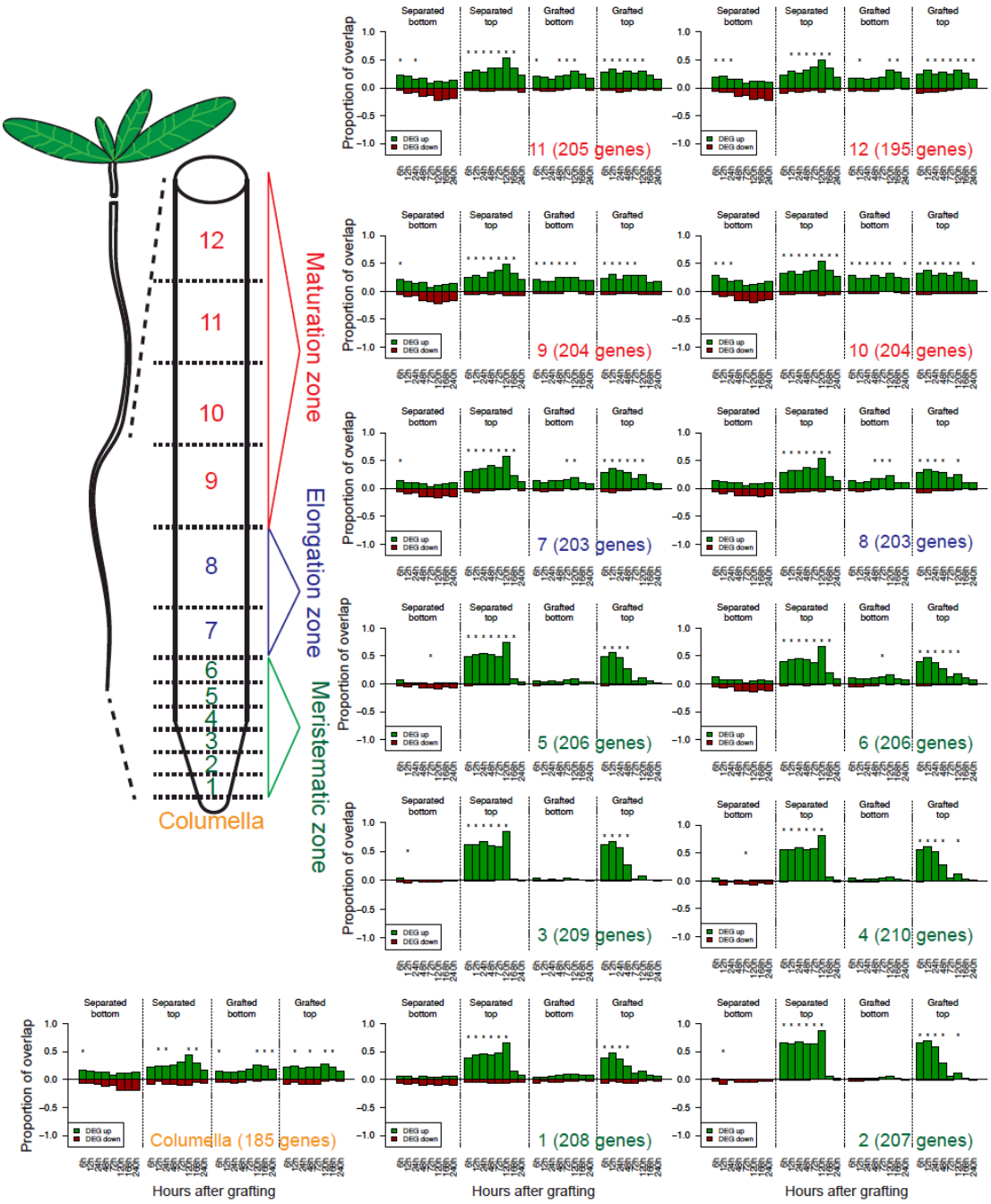

Figure S8. Transcriptional overlap between previously published root transcriptomic datasets and the grafting RNA-seq dataset, related to Figure 4. Genes whose transcripts are associated with various root regions were taken from previously published datasets (see Table S1) and compared to the datasets generated here. Root layer is indicated in the bottom right of each histogram with reference to the cartoon. The number in brackets represents the number of root layer-specific genes identified in the previous dataset, and overlap is presented as a ratio out of 1.0 for differentiation expressed genes (DEG) up- or down-regulated in our dataset relative to intact samples. Asterisks represent a significant difference ($p < 0.05$) between the ratio of up- and down- regulated genes in a previously published transcriptome dataset compared to the ratio of all up- and down- regulated genes in our grafting dataset at a certain time point.

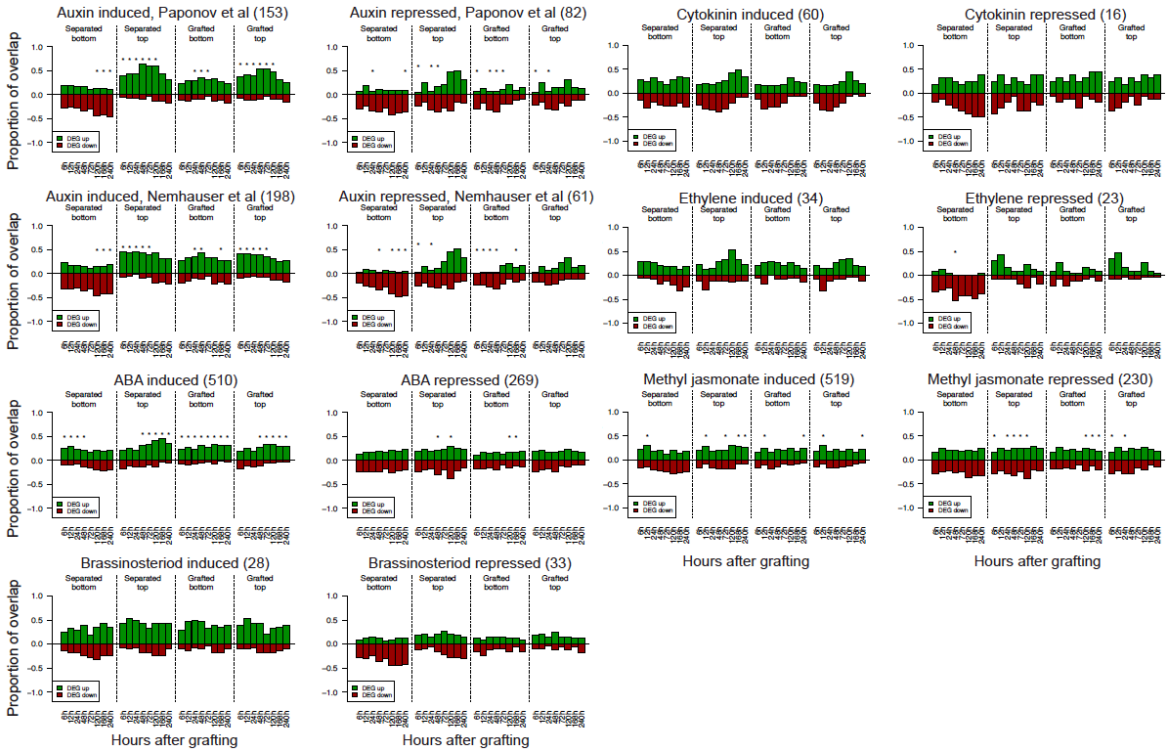

Figure S9. Transcriptional overlap between previously published hormone responsive RNA datasets and the grafting RNA datasets, related to Figure 5. Genes whose differential expression is associated with various hormone responses were taken from previously published datasets (see Table S1) and compared to the genes represented in the RNA-seq datasets generated. The number in brackets represents the number of cell type-specific or process-specific genes identified in the previous dataset, and overlap is presented as a ratio out of 1.0 for differentiation expressed genes (DEG) up- or down-regulated in our dataset relative to intact samples. Asterisks represent a significant difference ($p < 0.05$) between the ratio of up- and down- regulated genes in a previously published transcriptome dataset compared to the ratio of all up- and down- regulated genes in our grafting dataset at a certain time point.

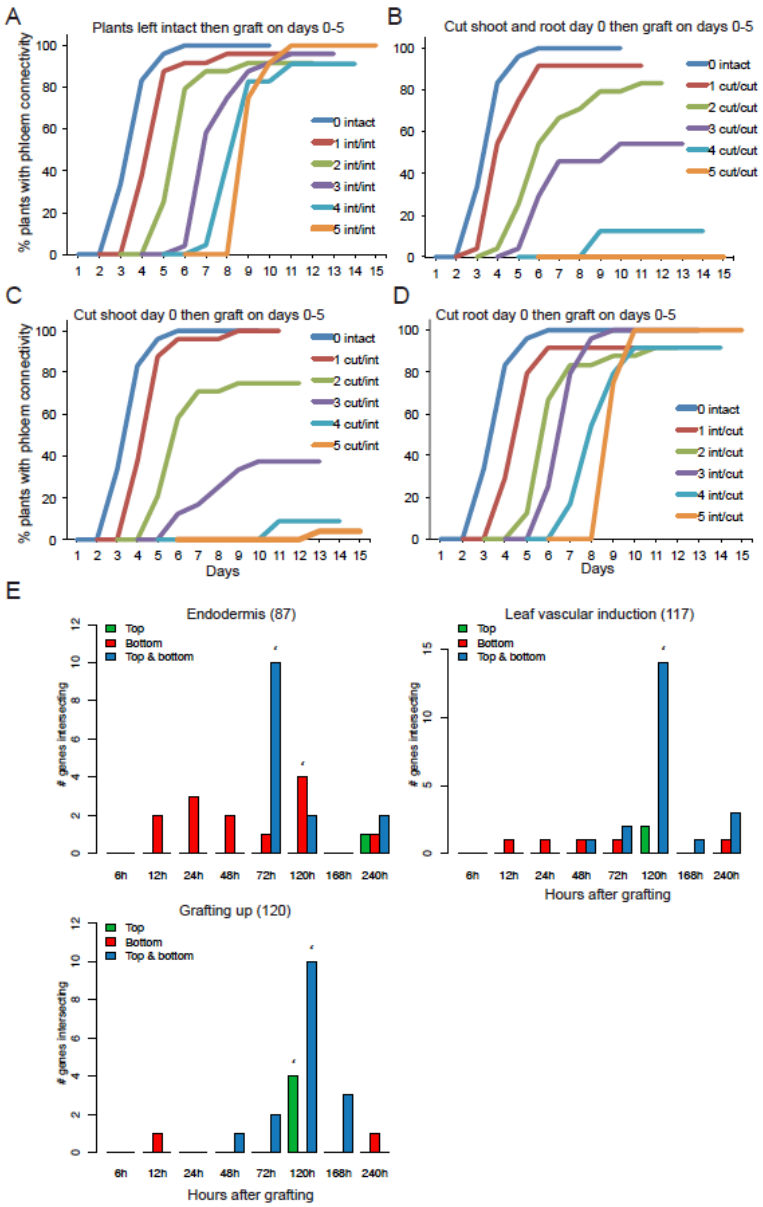

Figure S10. A subset of genes is differentially expressed only during graft formation, related to Figure 7. (A) *pSUC2::GFP* expressing *Arabidopsis* shoots were grafted to Col-0 wild type roots 0-5 days after transferring to grafting plates and kept intact until grafting (intact treatment). GFP movement to the roots for phloem connection assays was monitored over 7 days. (B) Plants were cut at day 0 and grafted at days 0-5 after cutting. (C) Shoots were cut at day 0 and grafted at days 0-5 after cutting. Roots were kept intact until immediately before grafting. (D) Roots were cut at day 0 and grafted at days 0-5 after cutting. Shoots were kept intact until immediately before grafting. (E) Genes differentially expressed in grafted tops and grafted bottoms show overlap with previously published genes whose transcripts are associated with the endodermis, vascular induction and grafting (see Table S1 for treatment information). Asterisks represent significant high overlap ($p < 0.05$) of previously published gene sets that are also differentially expressed in the grafted samples at a certain time point.